Measurement of the weak neutral form-factor of the proton at high momentum transfer

Kent Paschke
University of Virginia

E12-23-004

Spokespeople: R.Beminiwattha, D.Hamilton, C. Palatchi, KP, **B.Wojtsekhowski**

LaTech, Glascow, Indiana, UVa, JLab, CUA, INFN - Roma, Temple, Ohio, Syracuse, FIU, CNU, Fermilab, UWashington, Tel Aviv U, Hebrew U, W&M, AANL Yerevan, Northern Michigan, UConn, Orsay

Charge symmetry and the nucleon form factors

Charge Symmetry

$$G_E^p = \frac{2}{3}G_E^{u,p} - \frac{1}{3}G_E^{d,p}$$
$$G_E^n = \frac{2}{3}G_E^{u,n} - \frac{1}{3}G_E^{d,n}$$

Charge symmetry is assumed for the form factors, $G_E^{u,p} = G_E^{d,n}$, *etc.* and used to find the flavor separated form-factors, measuring $G_{E,M}^{p,n}$ to find $G_{E,M}^{u,d}$

$$G_E^p = \frac{2}{3}G_E^{u,p} - \frac{1}{3}G_E^{d,p} - \frac{1}{3}G_E^s$$
$$G_E^n = \frac{2}{3}G_E^{u,n} - \frac{1}{3}G_E^{d,n} - \frac{1}{3}G_E^s$$

But this can broken! One way is to have a non-zero strange form-factor, which breaks the "2 equations and 2 unknowns" system

The weak form factor provides a third linear combination:

$$G_E^{p,Z} = \left(1 - \frac{8}{3}\sin^2\theta_W\right)G_E^{u,p} + \left(-1 + \frac{4}{3}\sin^2\theta_W\right)G_E^{d,p} + \left(-1 + \frac{4}{3}\sin^2\theta_W\right)G_E^s$$

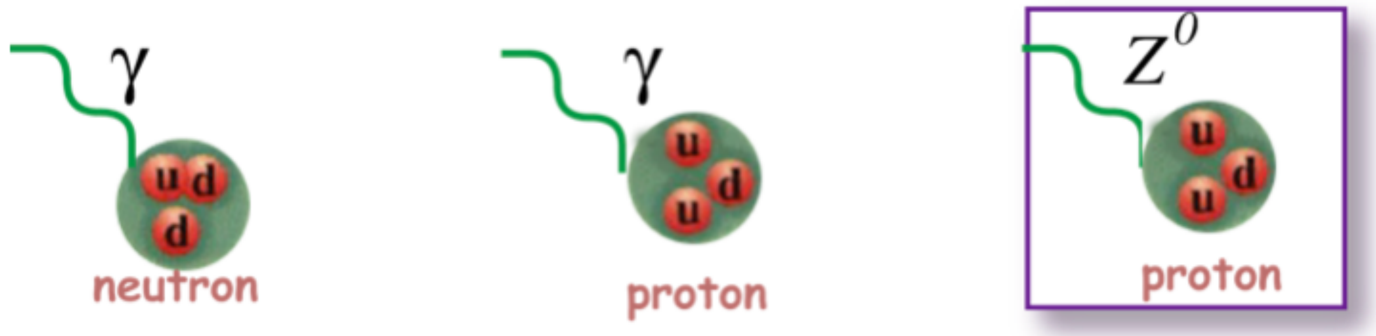

A strange quark form factor would be indistinguishable from a broken charge symmetry in u,d flavors

$$\delta G_E^u \equiv G_E^{u,p} - G_E^{d,n}$$
$$\delta G_E^d \equiv G_E^{d,p} - G_E^{u,n}$$

So, more generally: the assumption of charge symmetry is crucial to the flavor decomposition of the form factors

Strange Form Factors Are Not Shown To Be Zero

Flavor separation is required to understand nucleon structure implication of high-Q^2 form factors measurements

Based on charge symmetry, $u \leftrightarrow d$, but this is an untested assumption above Q^2~0.8 GeV^2

Earlier studies at low Q^2, typically more sensitive to G_E^s, do not extrapolate to a tight constraint at high Q^2

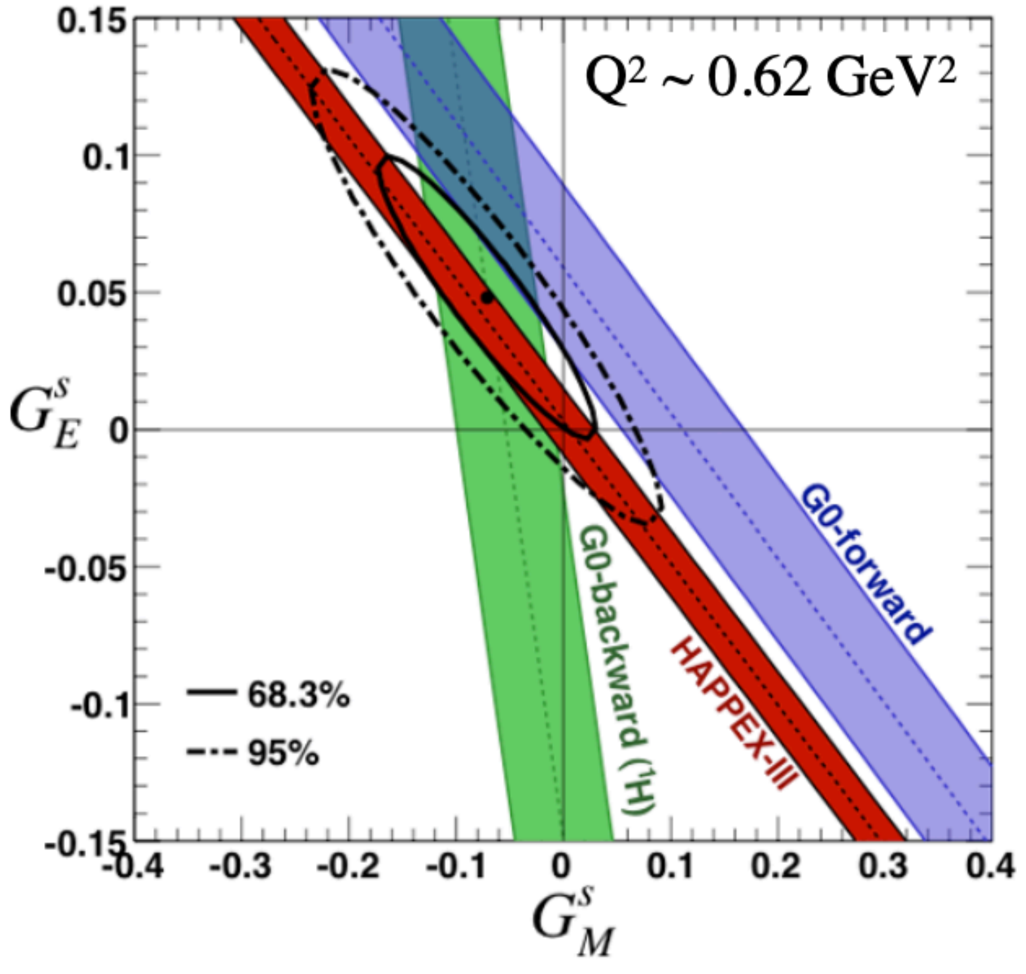

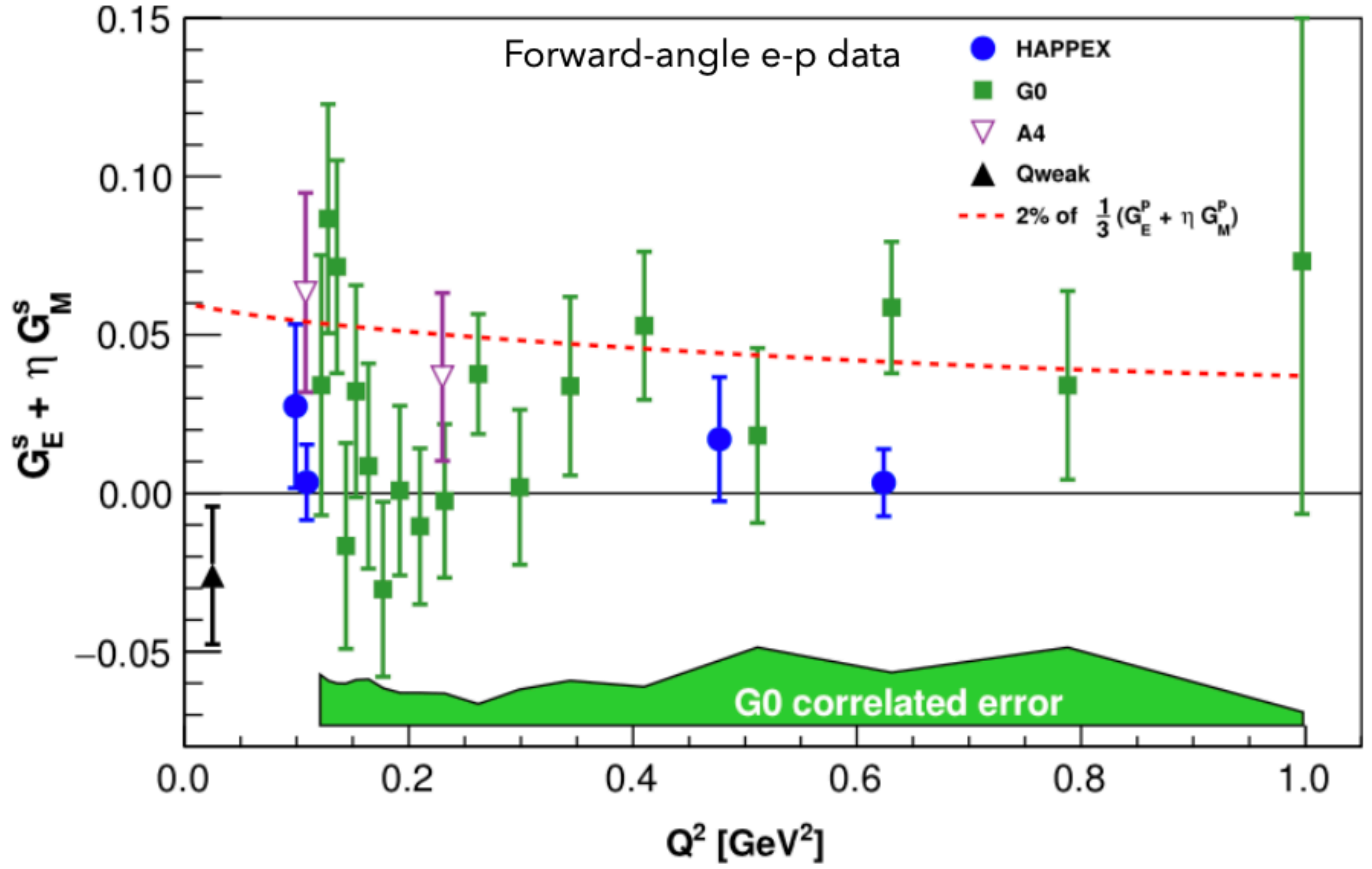

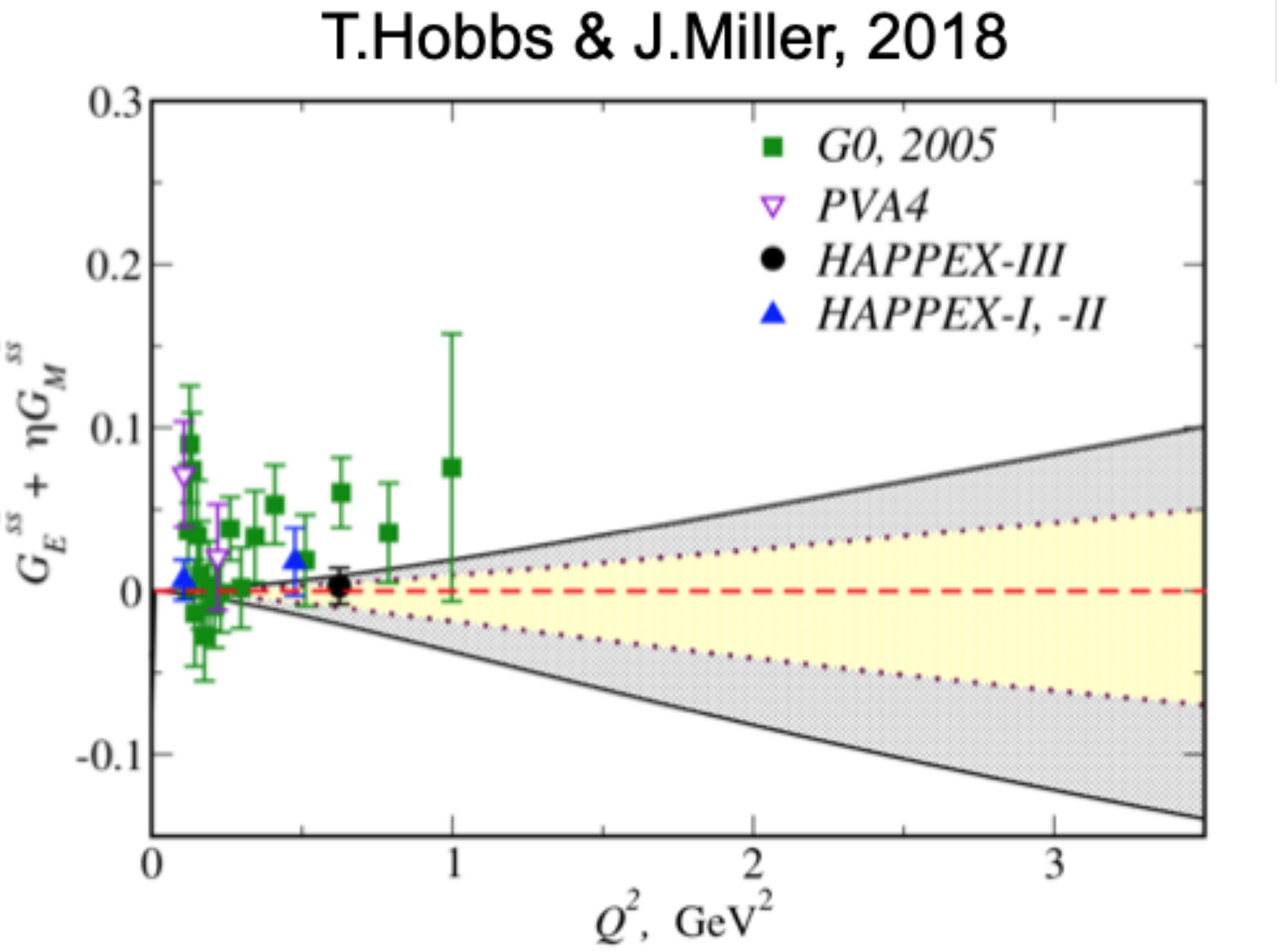

Hobbs & Miller, 2018: sFF small (but non-zero) at low Q^2, but within constraints from data may grow relatively large at large Q^2.

How large? Uncertainty band at Q^2~2.5 GeV^2 is about as large as $G_D(Q^2)$

Follows work from *Phys.Rev.C* 91 (2015) 3, 035205
(LFWF to tie DIS and elastic measurements in a simple model)

Strange form-factors on the lattice

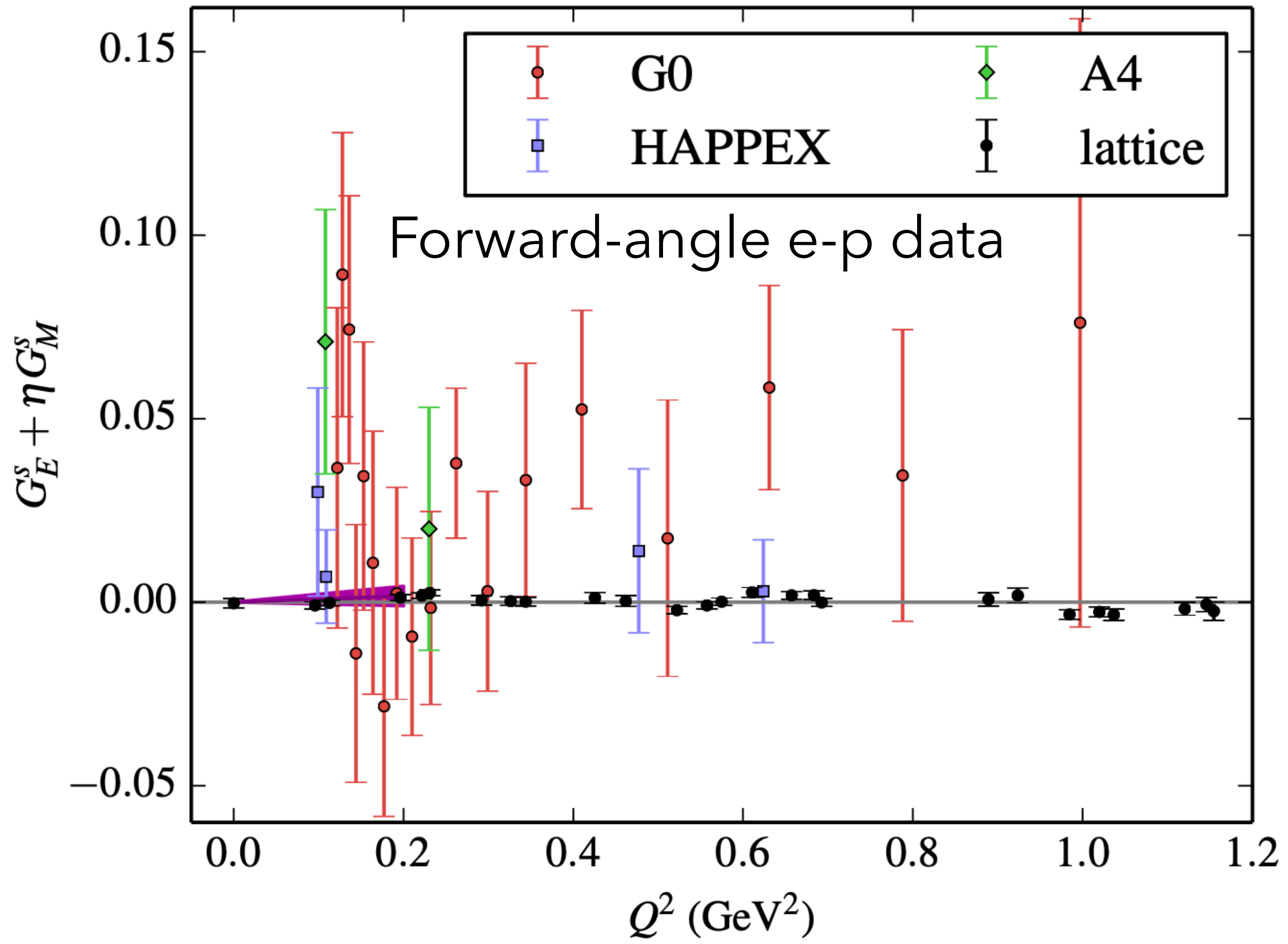

Even lattice results, which looked very small for low Q^2, do not reduce as fast as the dipole shape with Q^2

These values would be significant contributions at high Q^2

P. Shanahan *et al.*, PRL 114, 091802 (2015)

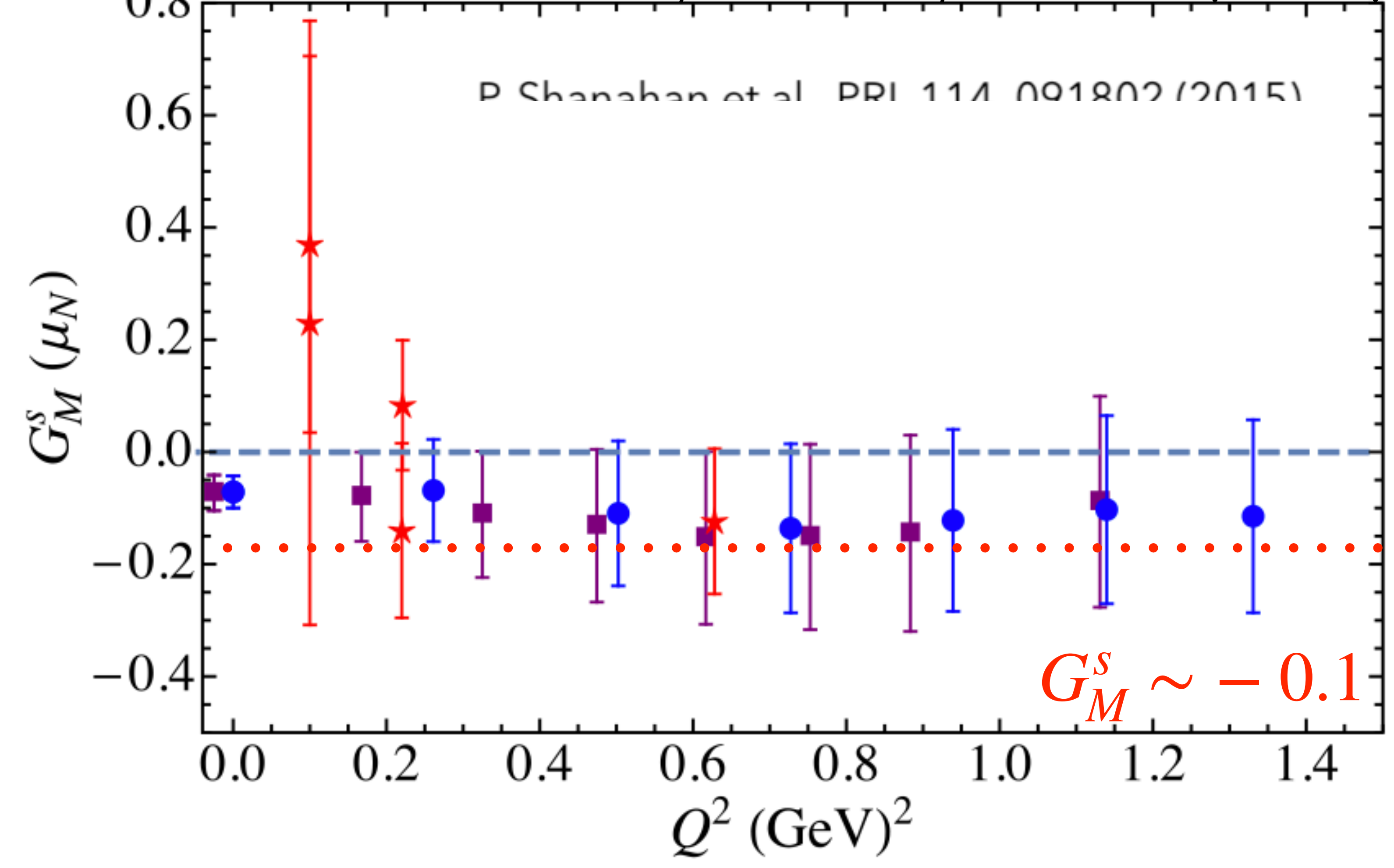

(a)

J. Green *et al.*, Phys. Rev. D 92, 031501 (2015)

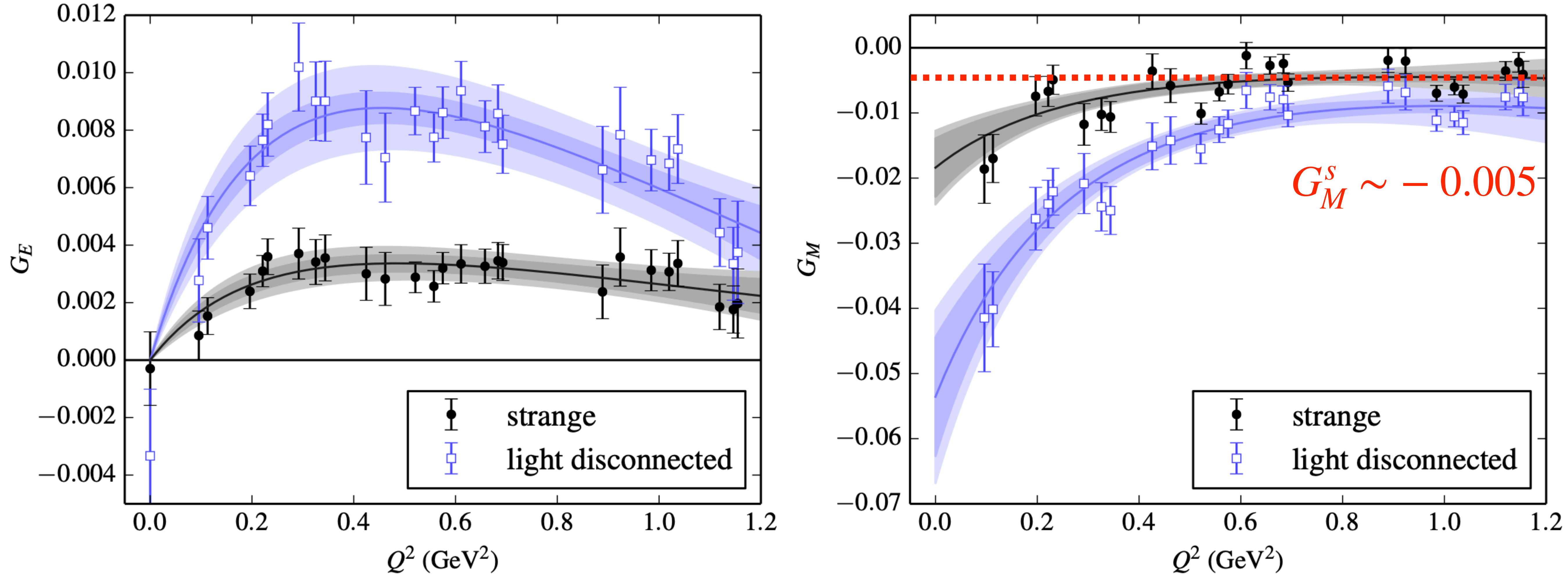

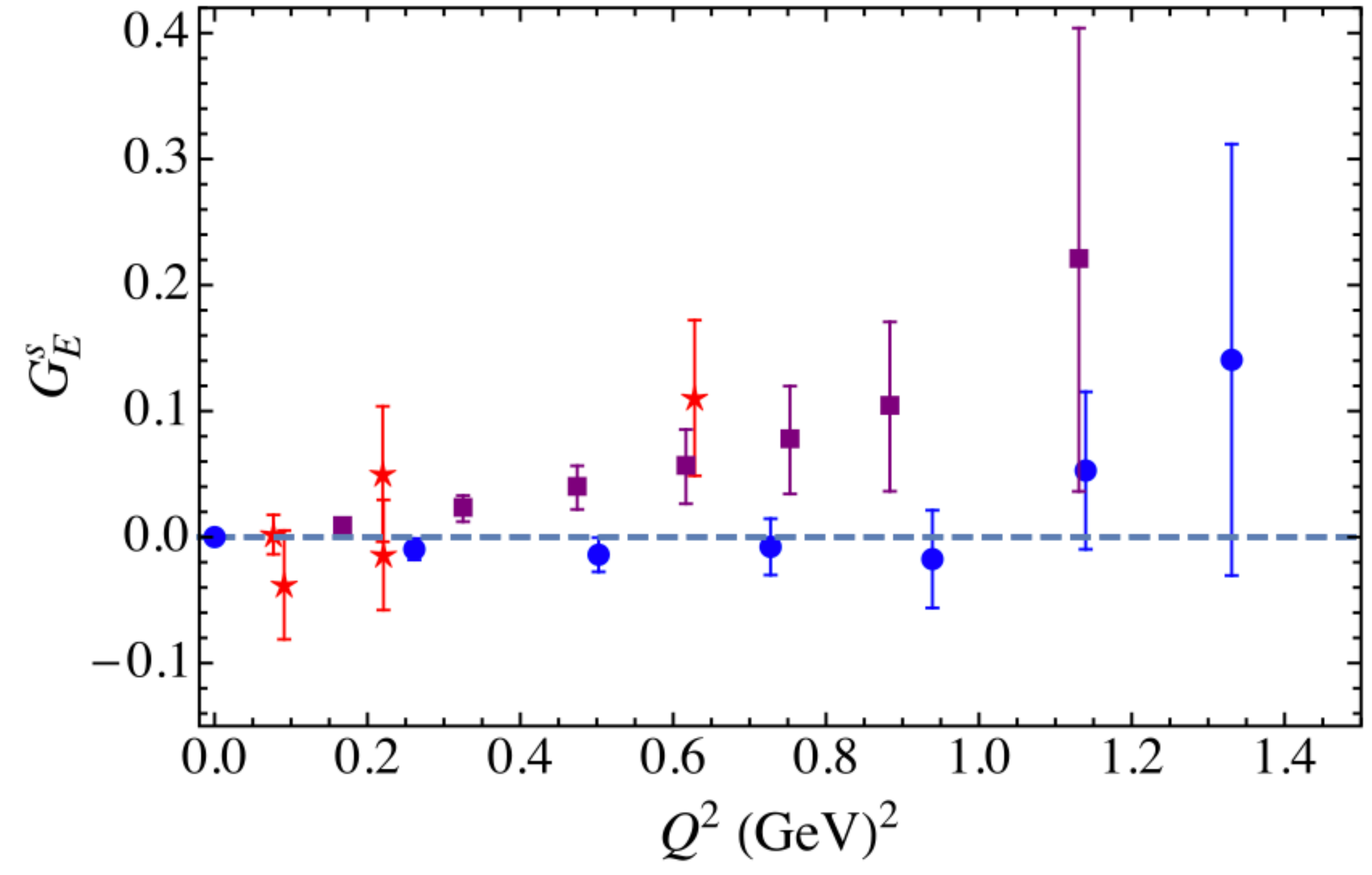

(b)

Parity Violating Electron Scattering

The weak neutral-current form-factor from parity violation can provide the required test of charge symmetry

Elastic e-p scattering with longitudinally polarized beam and unpolarized target:

Weak and EM amplitudes interfere:

$$\boxed{\sigma = |\mathcal{M}_\gamma + \mathcal{M}_Z|^2}$$

$$A_{PV} = \frac{\sigma_R - \sigma_L}{\sigma_R + \sigma_L} \sim$$

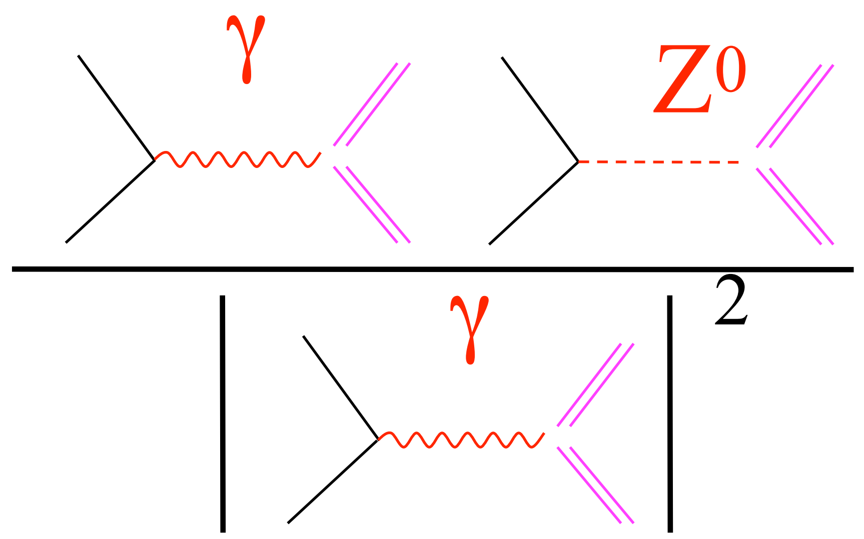

$$\approx \frac{|\mathcal{M}_Z|}{|\mathcal{M}_\gamma|}$$

Expressing A_{PV} for e-p scattering, with proton and neutron EM form-factors plus strange form factors:

$$A_{PV} = -\frac{G_F Q^2}{4\pi\alpha\sqrt{2}} \cdot [(1-4\sin^2\theta_W) - \frac{\epsilon G_E^p G_E^n + \tau G_M^p G_M^n}{\epsilon (G_E^p)^2 + \tau (G_M^p)^2} - \frac{\epsilon G_E^p G_E^s + \tau G_M^p G_M^s}{\epsilon (G_E^p)^2 + \tau (G_M^p)^2}$$
$$+ \epsilon'(1-4\sin^2\theta_W)\frac{G_M^p G_A^{Zp}}{\epsilon (G_E^p)^2 + \tau (G_M^p)^2}]$$

Previous studies were focused particularly on the *static* (*i.e.* $Q^2 \rightarrow 0$) properties: a strange charge radius or strange magnetic moment. Precision at larger Q^2 requires a new approach.

The planned measurement

Aim for $Q^2 = 2.5\ GeV^2$

Identify elastic kinematics with electron-proton coincidence

- Angular e-p correlation
- High resolution calorimeter for electron trigger
- Calorimeter for proton trigger
- Scintillator array on proton arm, to improve position resolution

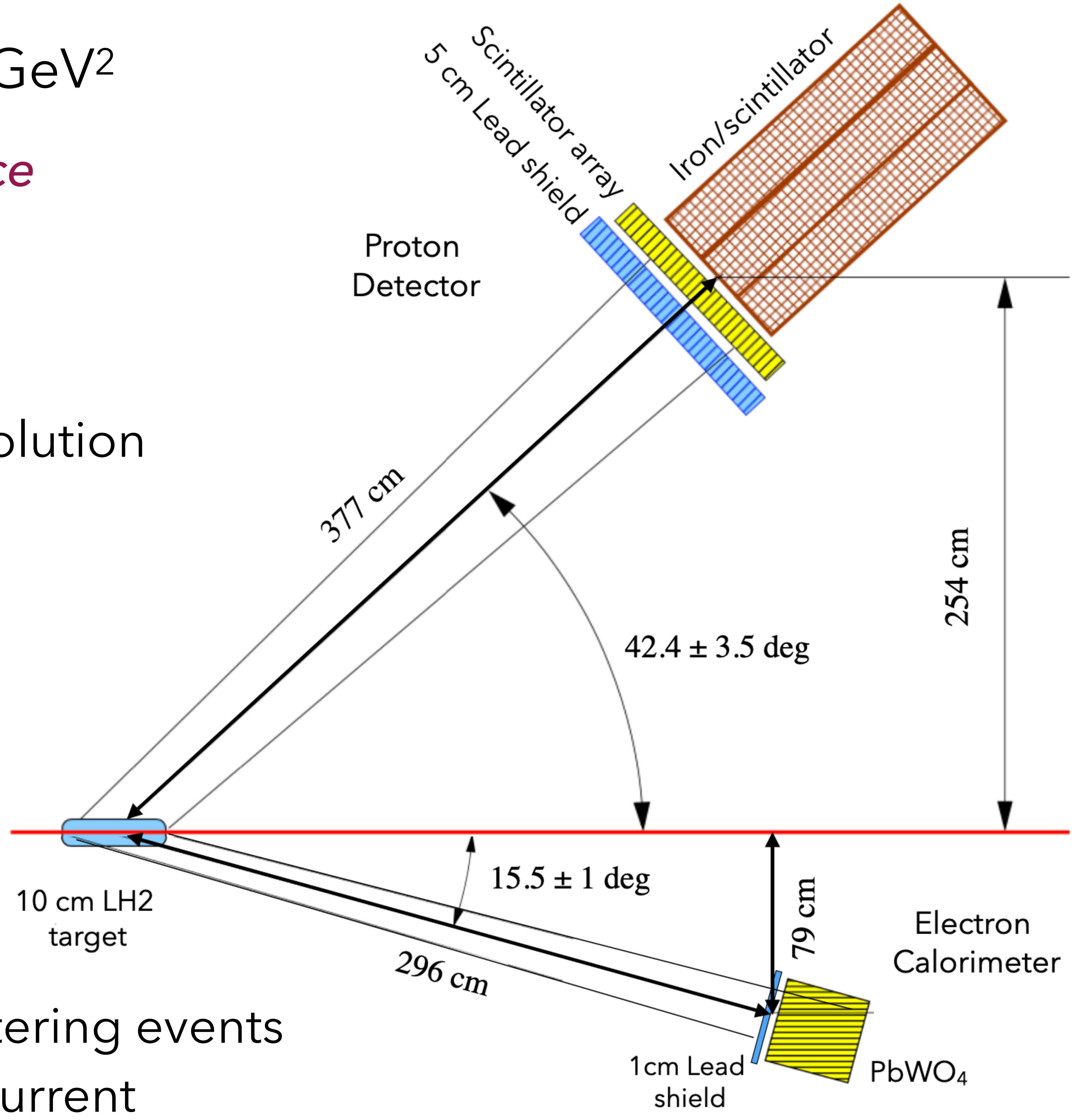

- 6.6 GeV beam energy
- electron at 15.5 degrees, proton at 42.4 degrees
- A_{PV} = 150 ppm, 4% precision goal, so 3×10^{10} elastic scattering events
- $\mathcal{L} = 1.7 \times 10^{38}\ cm^{-2}/s$, 10 cm LH_2 target and 65 μA beam current
- Full azimuthal coverage, ~42 msr

Experimental concept

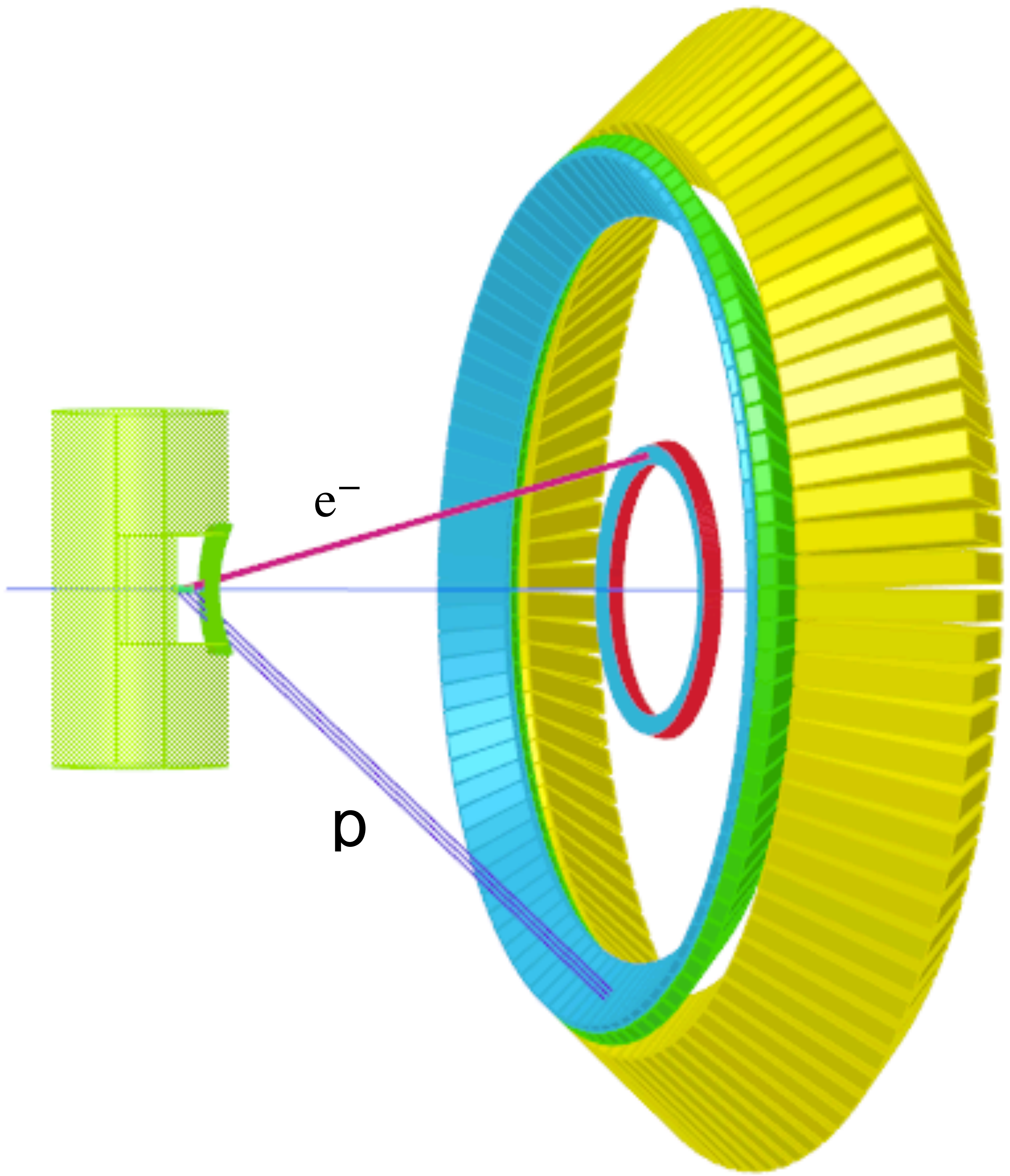

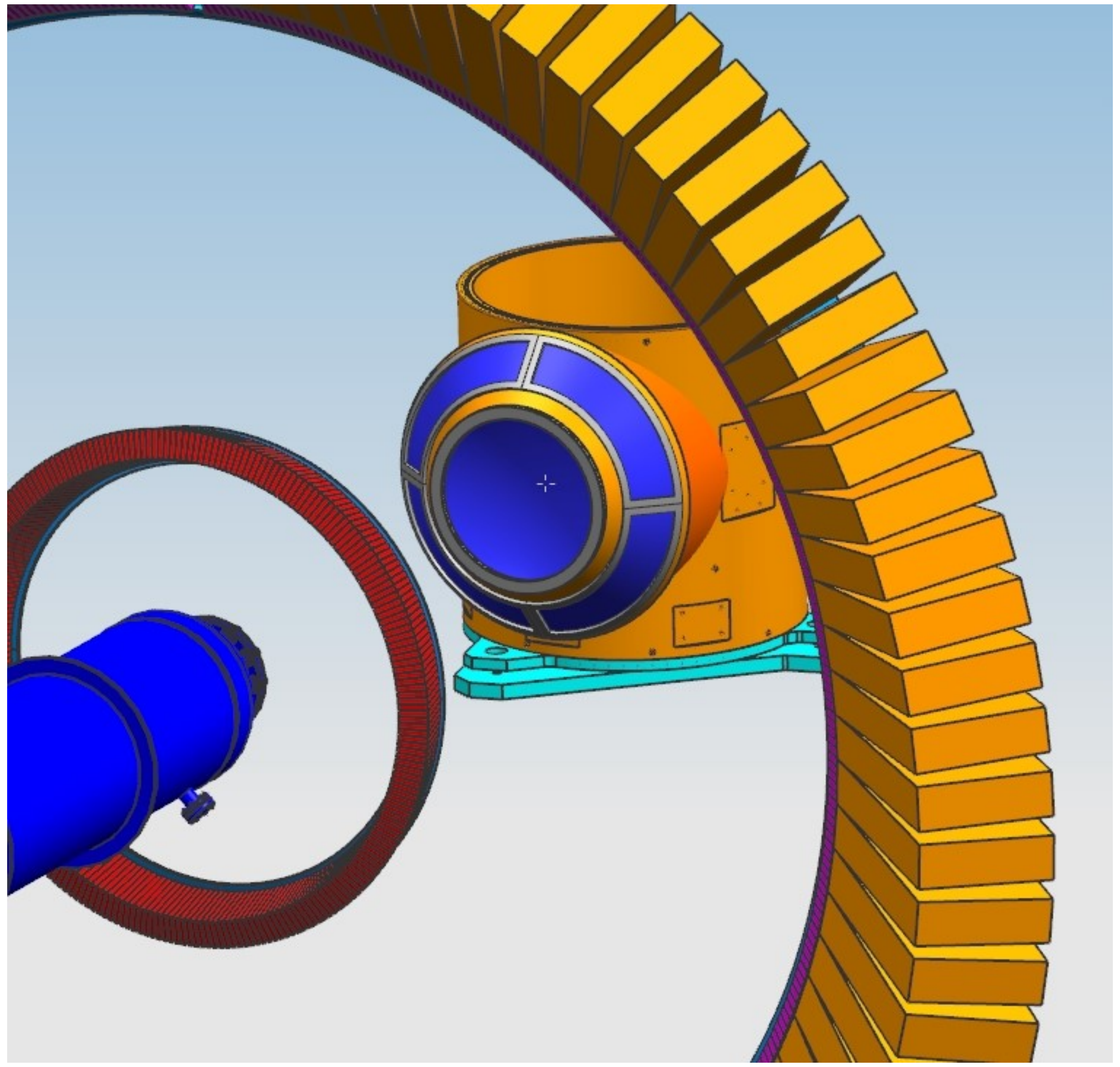

Preliminary design of scattering chamber

He bag will reduce backgrounds between target chamber and exit beampipe

This fits in Hall C (but it's tight)

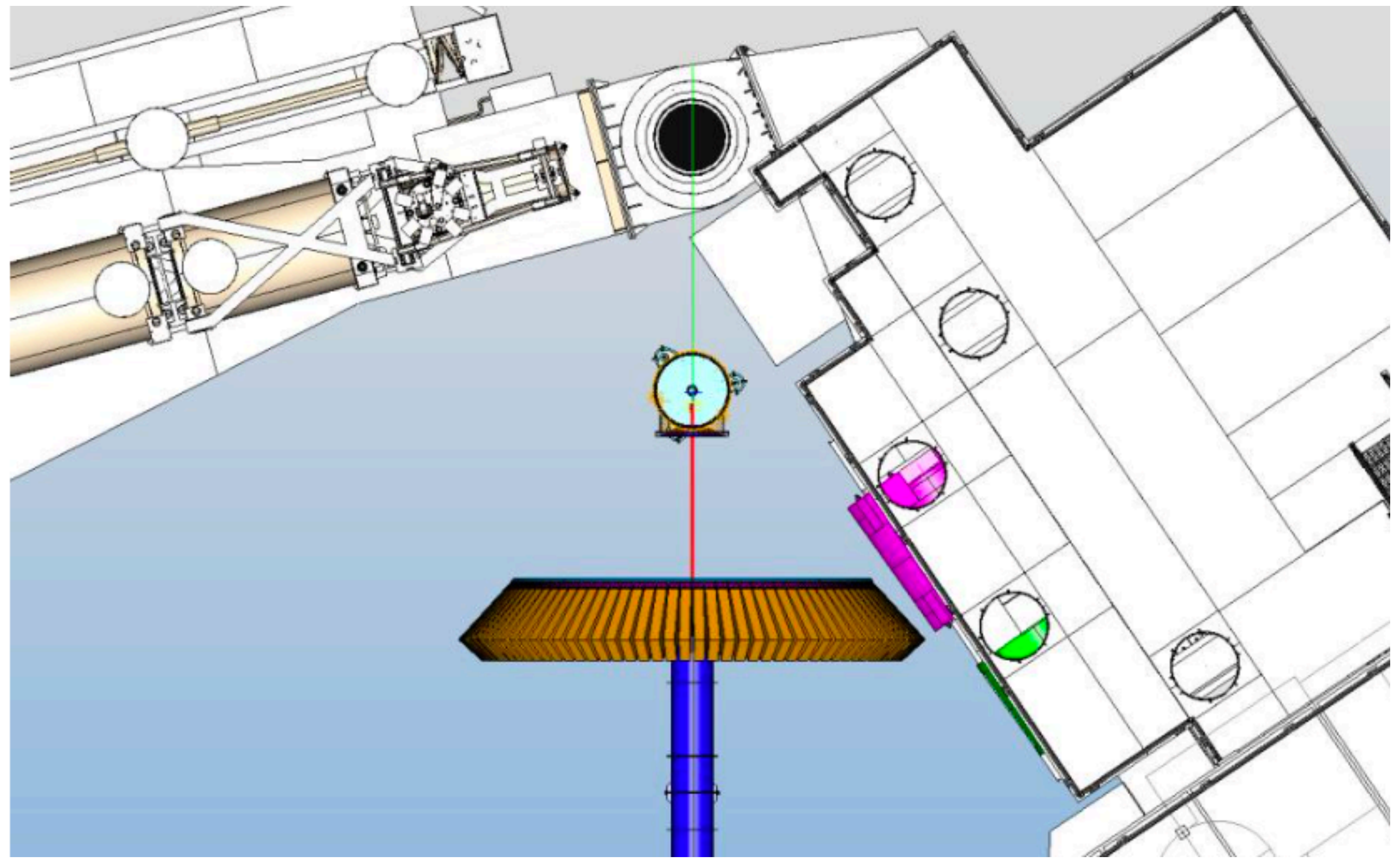

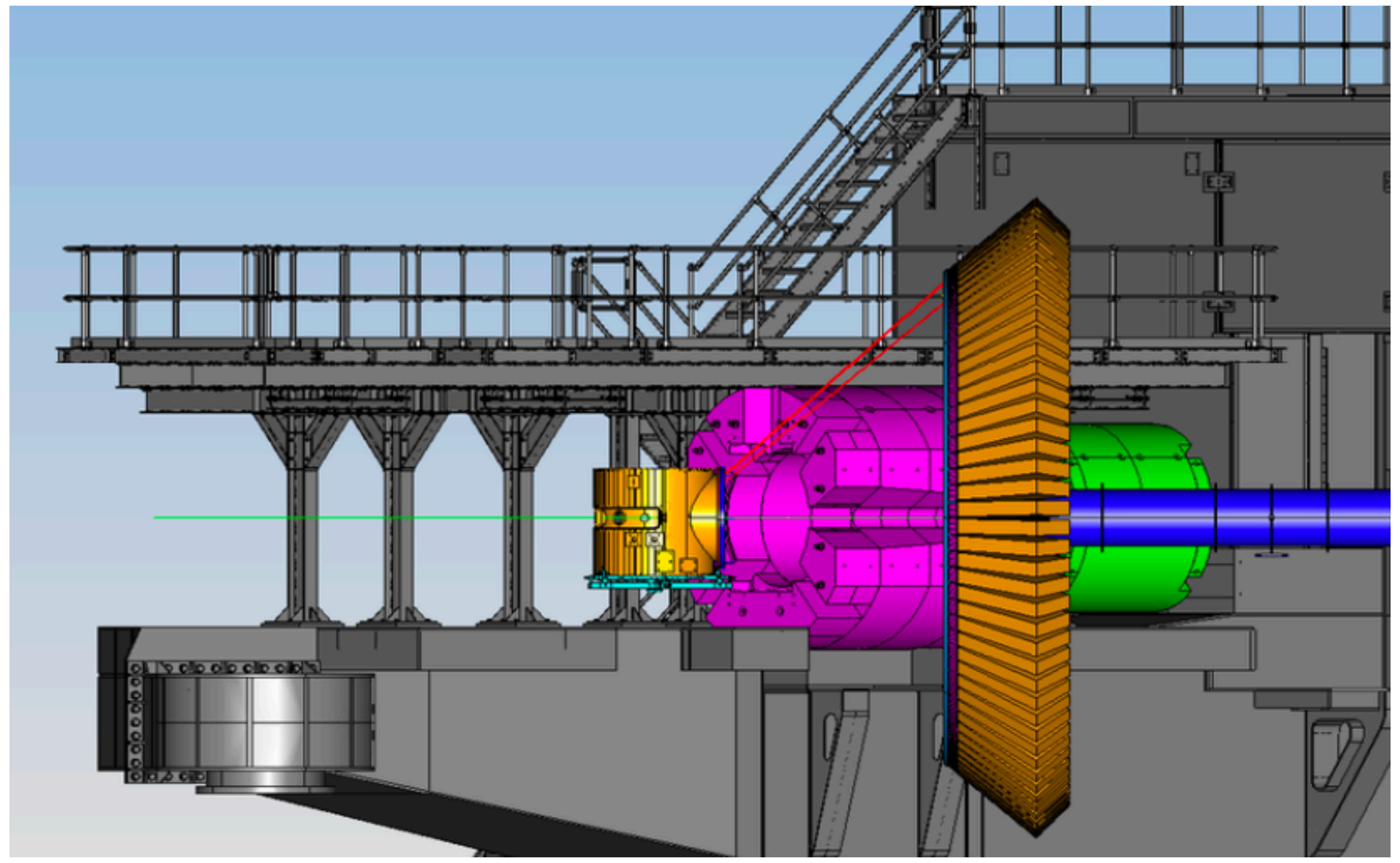

Detector System

HCAL - hadron calorimeter

- Detector elements from the SBS HCAL
- 288 blocks, each 15.5 x 15.5 x 100 cm^3
- iron/scintillator sandwich with wavelength shifting fiber readout

ECAL - electron calorimeter

- Detector elements from the NPS calorimeter
- 1200 blocks, each 2 x 2 x 20 cm^3
- $PbWO_4$ scintillator

Scintillator array

- 7200 plastic scintillators, each 3 x 3 x 10 cm^3
- Wavelength shifting fiber to MA-PMT
- Needed for position resolution at HCAL

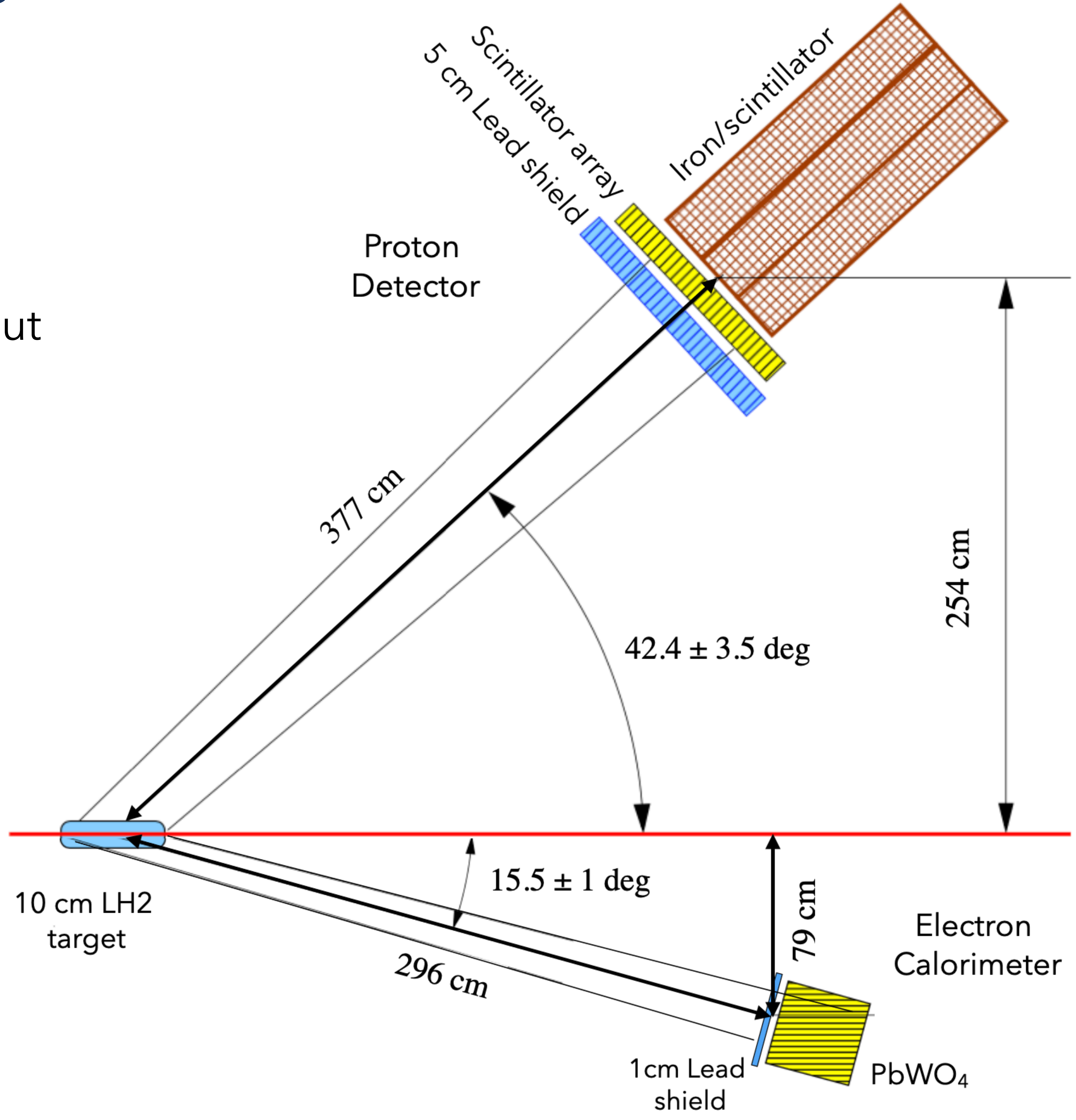

Fast Counting DAQ

250 MHz flash ADC (JLab **FADC250**) for HCAL and ECAL readout
Provides the pulse information for a fast, "deadtime-less" trigger

VTP (VXS Trigger Processor)
Running, updating sums over overlapping calorimeter clusters, to find ECAL+HCAL coincidence above threshold

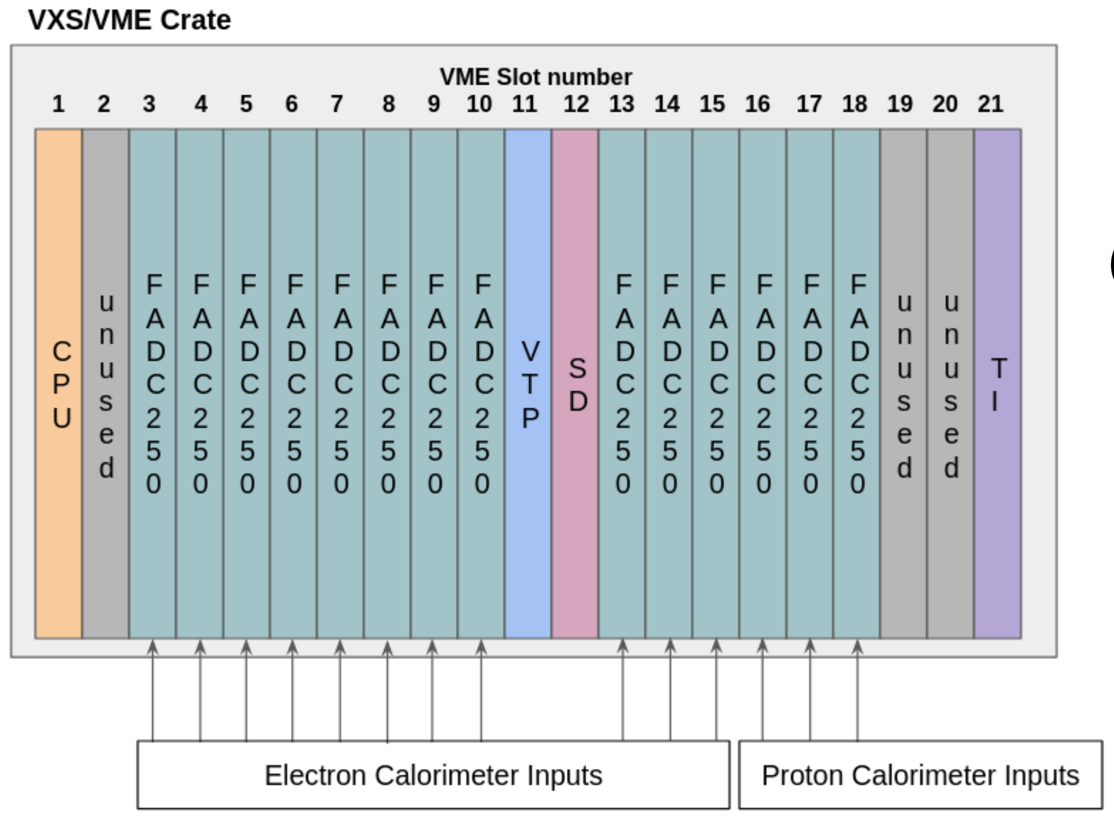

One VXS crate will handle one sixth of ECAL + HCAL, also provide external trigger for ScintArray pipelineTDC readout

Corresponding scintillator elements recorded in TDC (pulse time, time over threshold) with each trigger

Expect ~35kHz total, ~500 Mb/s data rate,
distributed over 6 separate crates (calorimeters) and 3 crates for scintillators

Trigger: calorimeters, with geometric coincidence

A relatively high ECAL cut (~66% of beam energy) and loose e-p coincidence cut provides high efficiency and manageable data rate

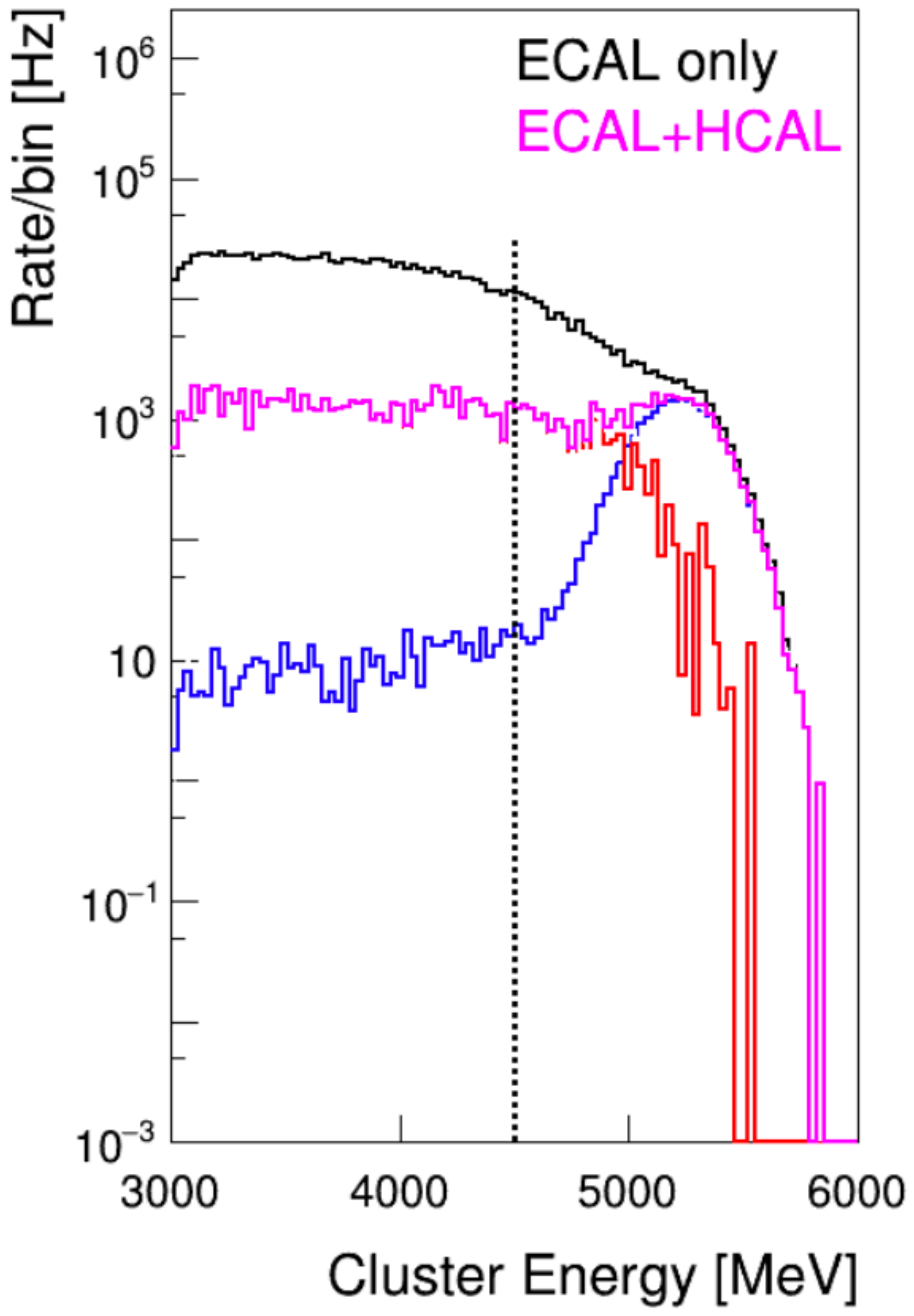

ECAL > 4.5 GeV: 150 kHz

ECAL + HCAL in coincidence: 35 kHz

Fraction of total by event type	Online
Elastic scattering	0.531
Inelastic (pion electro-production)	0.450
Quasi-elastic scattering (target windows)	0.015
π^0 photo-production	0.004

Elastic event discrimination

Azimuthal angle

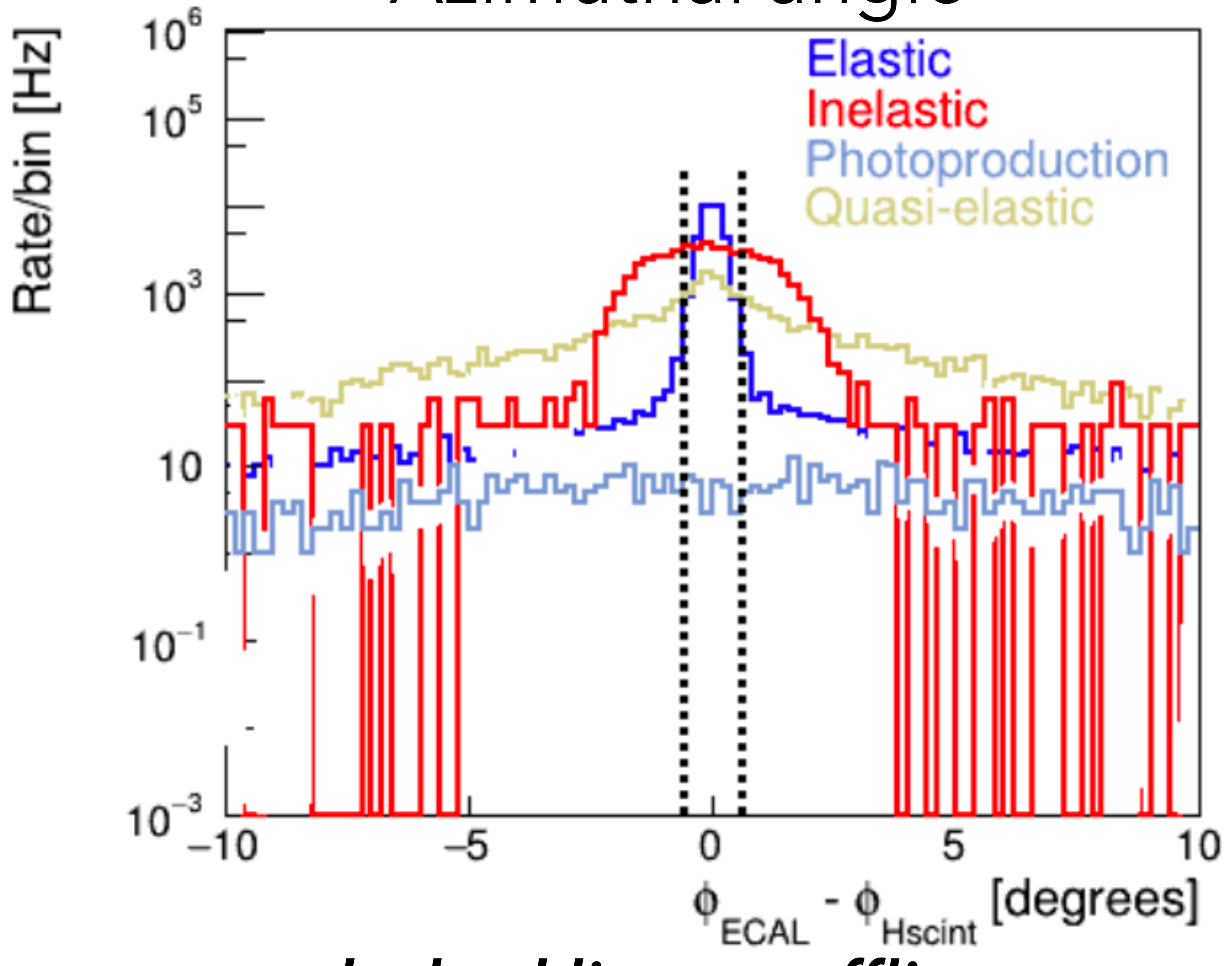

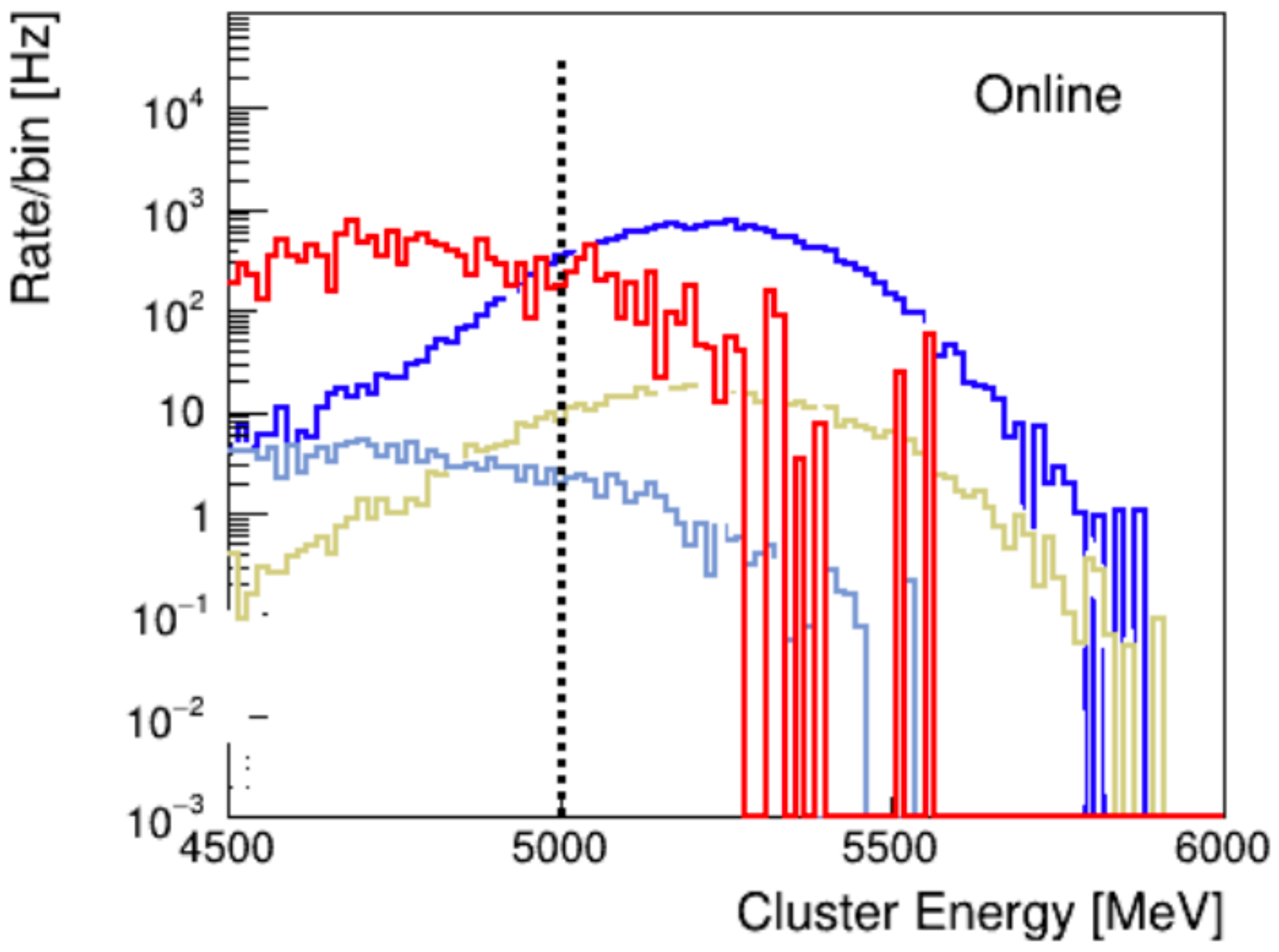

dashed lines = offline cuts

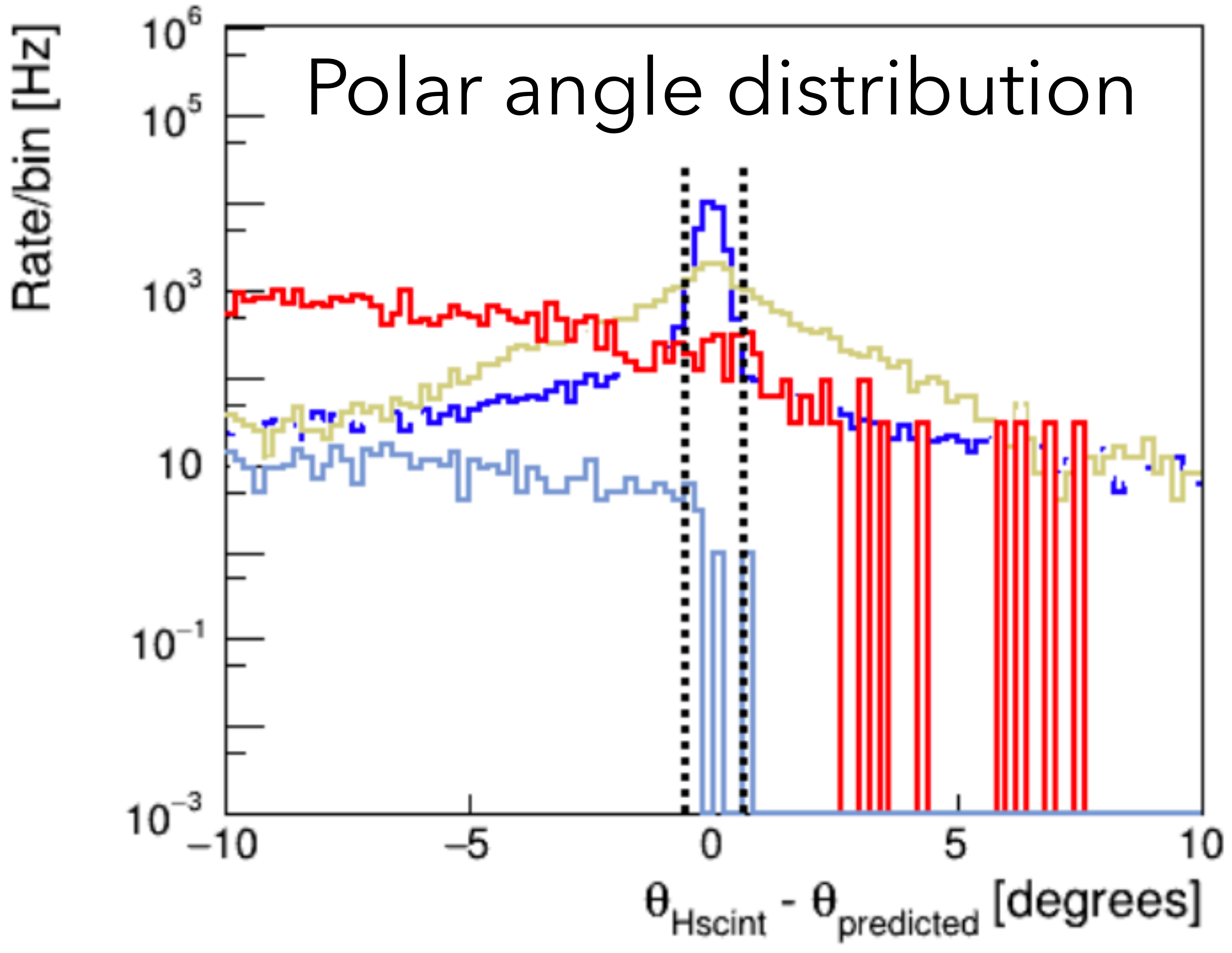

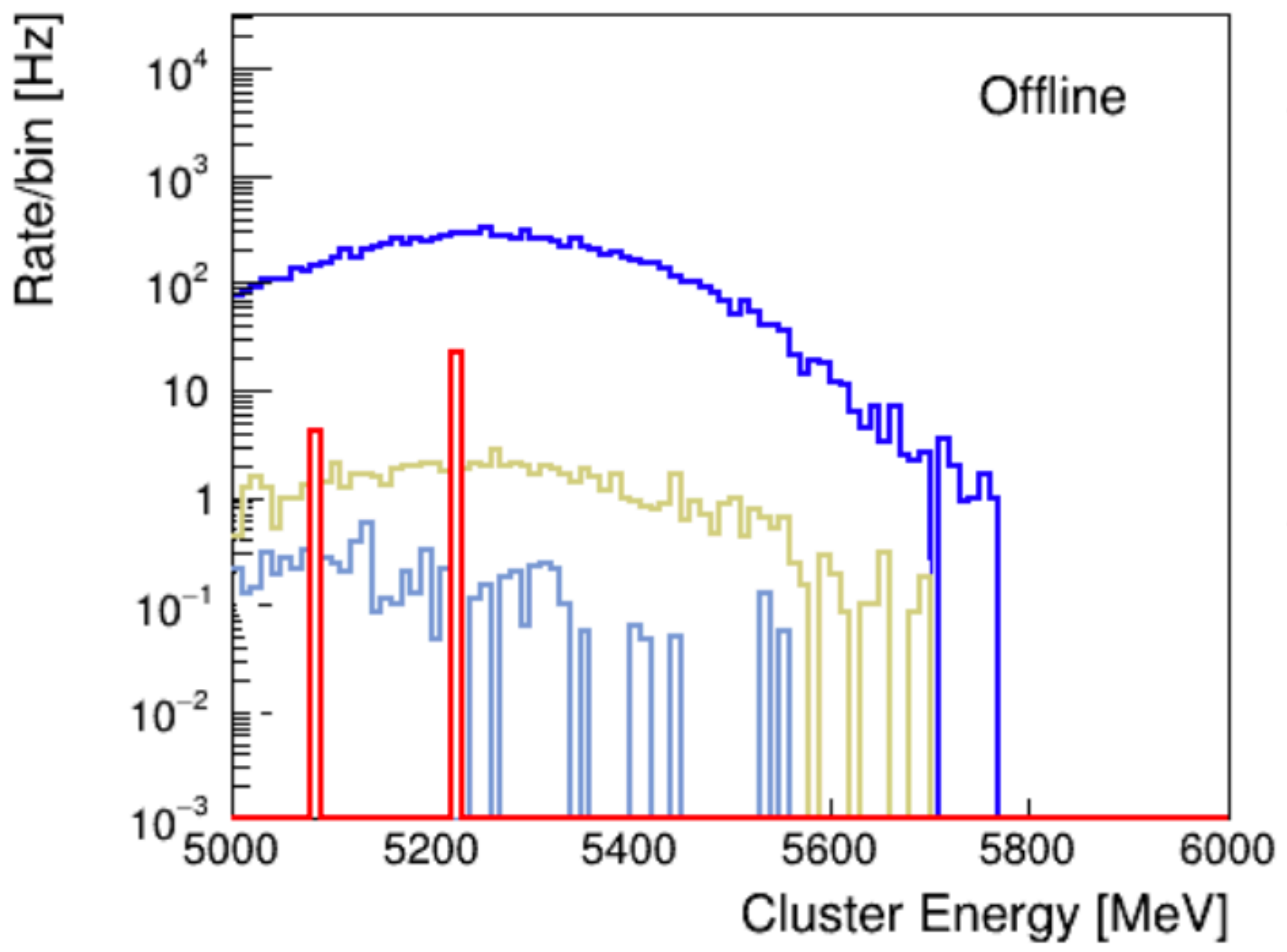

Online: ECAL vs HCAL coincidence, loose time and geometric cut

Offline: tighten geometric cut with pixel hodoscope and ECAL cluster center

Exclude inelastic background to ~0.2%

Fraction of total by event type	Offline
Elastic scattering	0.989
Inelastic (pion electro-production)	0.002
Quasi-elastic scattering (target windows)	0.008
π^0 photo-production	0.001

“sideband” analyses will help verify QE and inelastic asymmetries

Projected result

A_{PV} = 150 ppm (if no strange FF)

δA_{PV} = ± 6.2 (stat) ± 3.3 (syst) ($\delta A/A$ = ± 4% ± 2%)

$$\delta\left(G_E^s + 3.1 G_M^s\right) = \pm\ 0.013\ \text{(stat)}\ \pm\ 0.007\ \text{(syst)} = 0.015\ \text{(total)}$$

$$\frac{\text{SFF}}{\eta} = G_E^s + \frac{\tau G_M^p}{\epsilon G_E^p} G_M^s$$

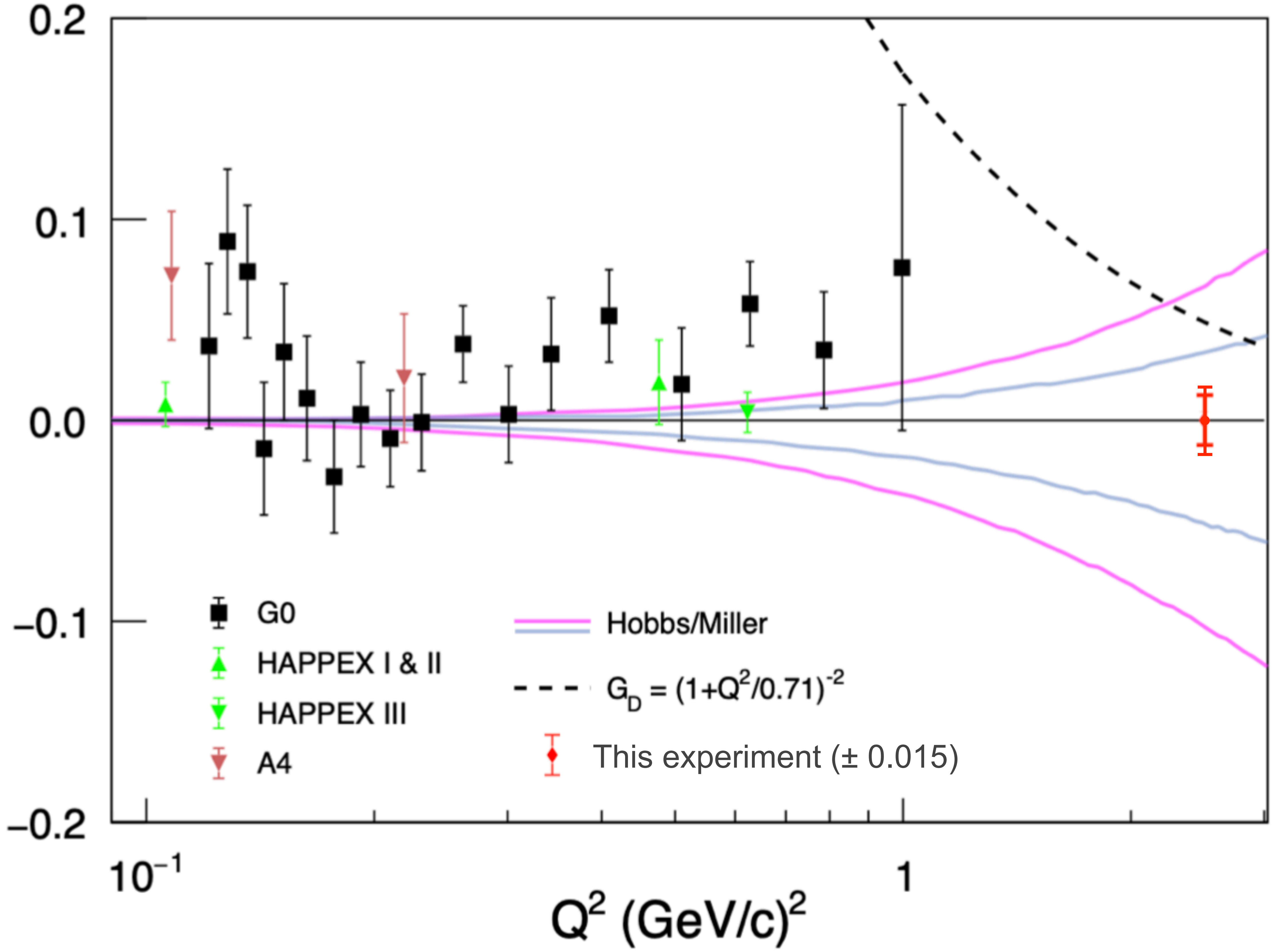

If $G_M^s = 0$, $\delta G_E^s \sim 0.015$, (about 34% of G_D)

If $G_E^s = 0$, $\delta G_M^s \sim 0.005$, (about 11% of G_D)

The proposed measurement is especially sensitive to G_M^s

The proposed error bar reaches the range of lattice predictions, and the empirically unknown range is much larger.

Next Step - Test Performance of Detector Concept

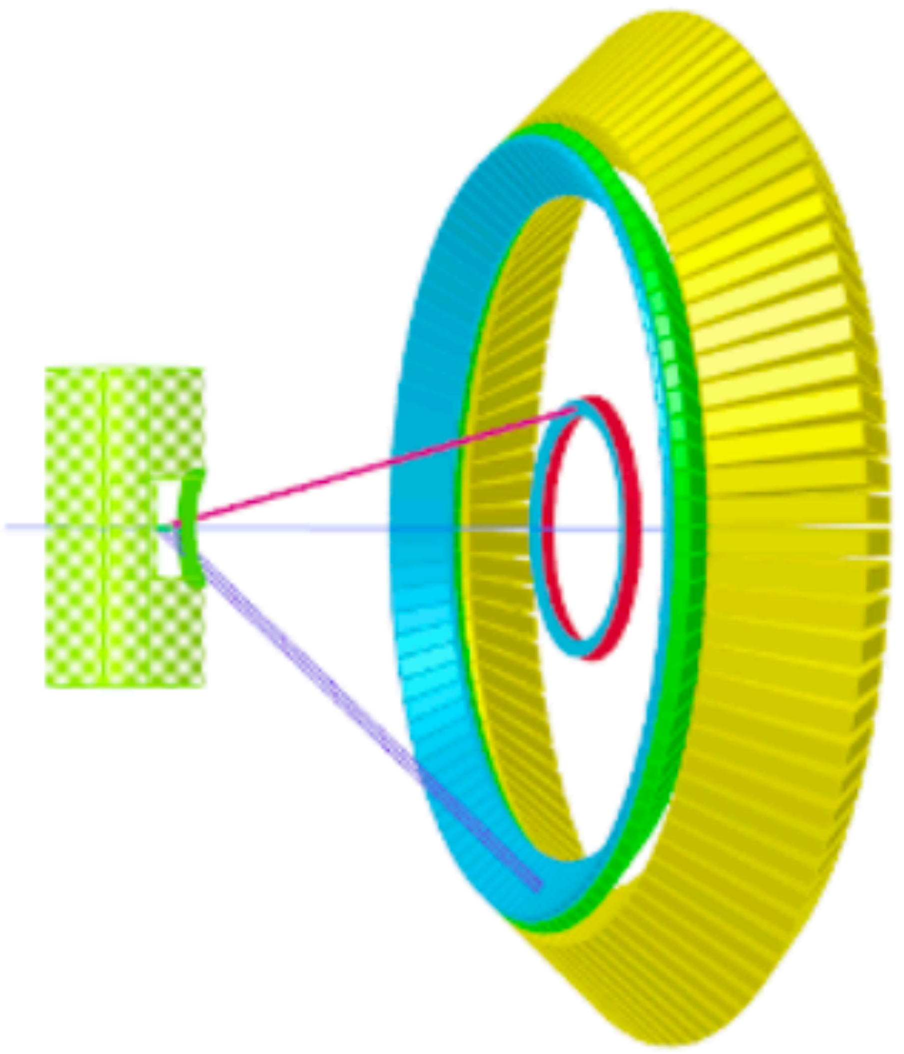

electron angle 15.5°
proton angle 42.4°

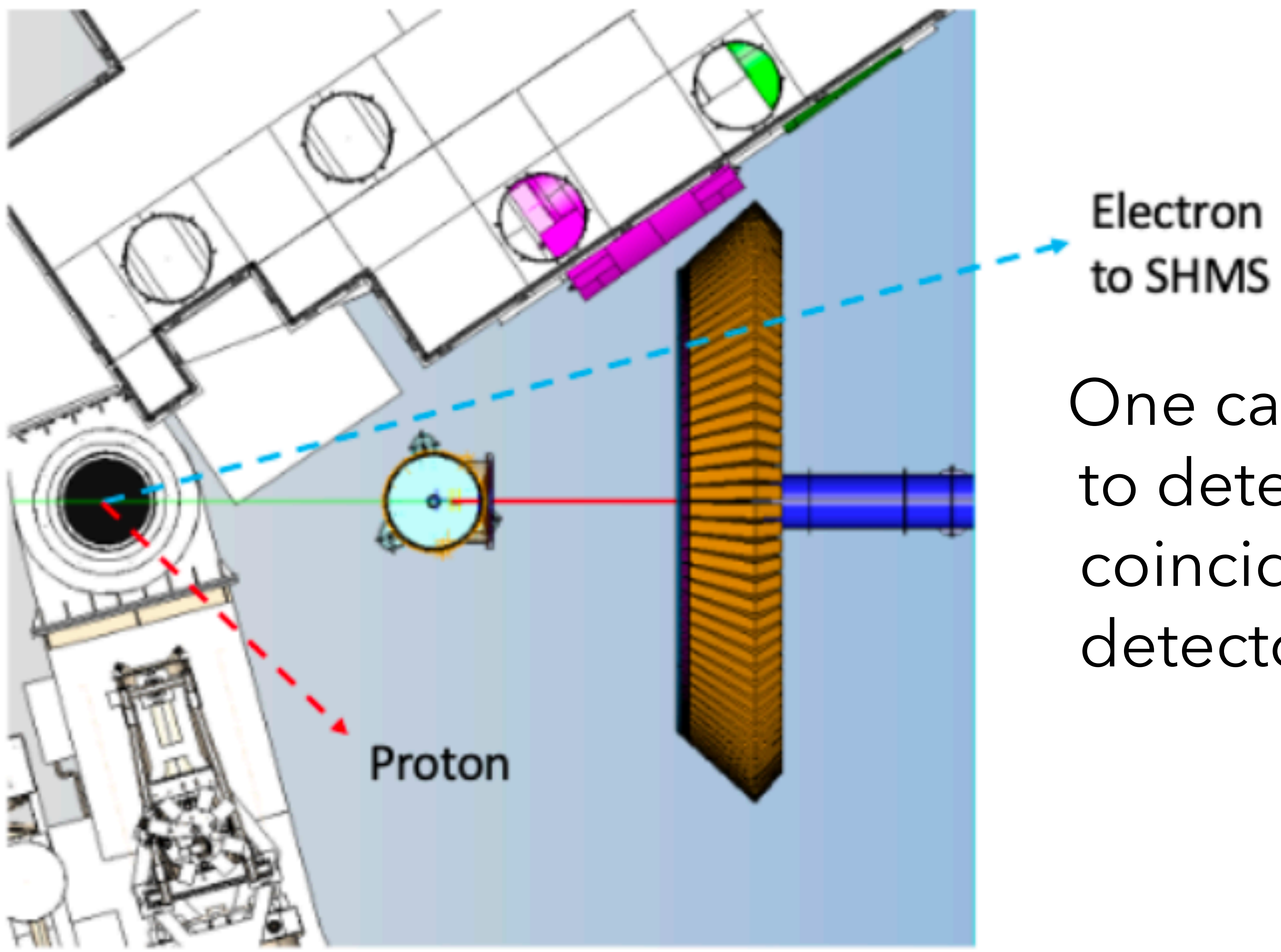

One can position the SHMS to 15.5° to detect electrons, measured in coincidence with a prototype proton detector at 42.4°

Prototype proton detector:

- pixel array of 20 small scintillators with MA-PMT readout + 2x2 SBS HCAL blocks
- FADC readout in spectrometer DAQ
- 50uA on 15cm Hydrogen target at 6.6 GeV, about 2kHz rate into detector
- test elastic identification and background rate and exclusion

prototype scintillator at JLab for assembly

"sFF" Strange Form Factors at High Q^2

10+ years after the last sFF searches were performed, a new experiment is now planned for much higher Q^2, motivated by interest in flavor decomposition of electromagnetic form factors

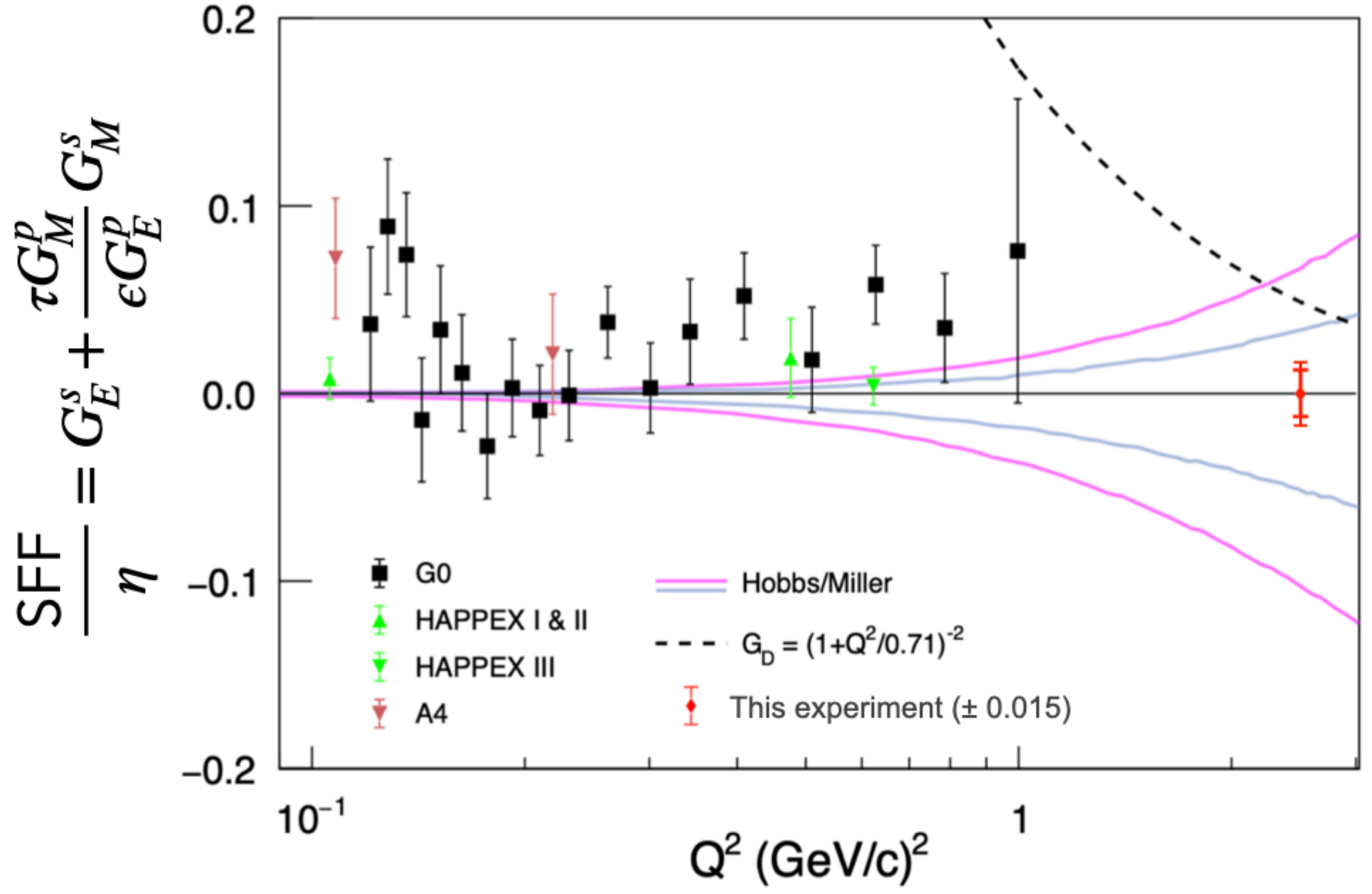

Progress, but significant work still to be done toward beam test

- scintillator array prototype construction (soon to start)
- assemble and test HCAL prototype
- simulation to select proton arm location
- mechanical design of proton arm test stand
- Detail DAQ configuration and prepare analysis

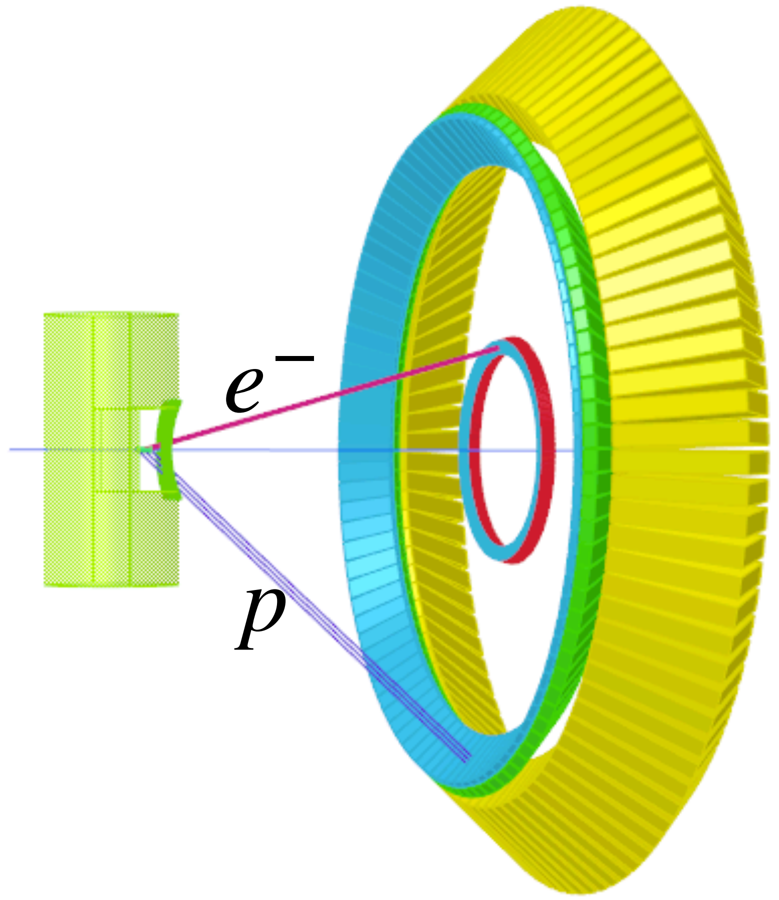

Backup slides

Triggering

Group calorimeter elements into logical "subsystems" for energy threshold and coincidence triggering

- each polar column of detectors, overlapping with neighbors
- sum amplitude with conservative coincidence timing window
- compare to conservative energy threshold
- trigger when complementary (ECAL and HCAL) subsystems are both above threshold ~ only about 35 kHz

Electron subsystems

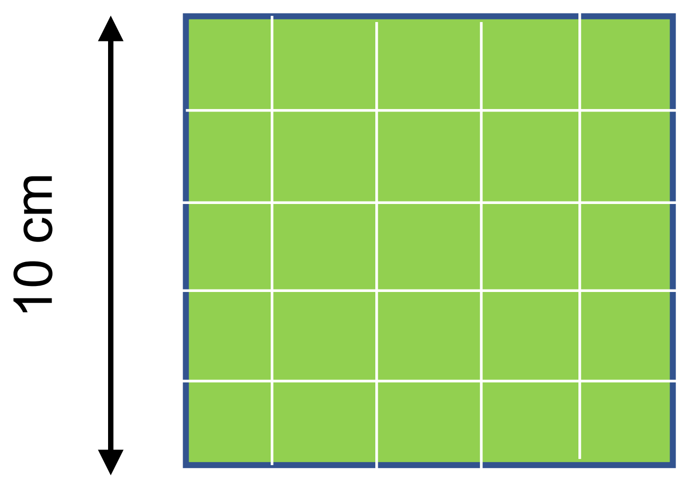

- 1200 $PbWO_4$ crystals
- 2x2x20 cm^3
- 5x5 grouping for subsystem
- 240 overlapping subsystems

Proton subsystems

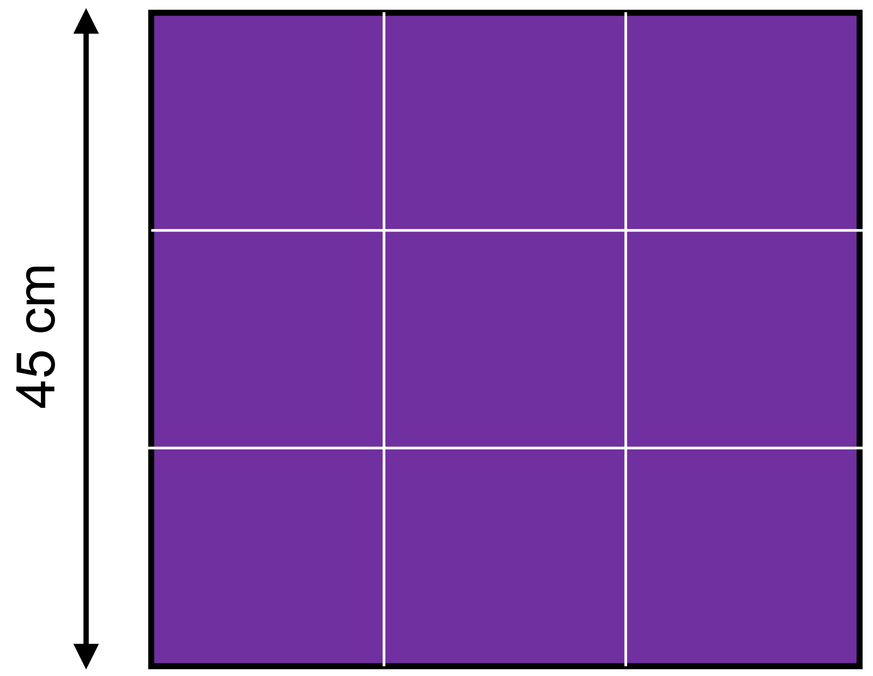

- 288 iron/scintillators
- 15.5x15.5x100 cm^3
- 3x3 grouping for subsystem
- 96 overlapping subsystems

Advantage: simplicity over dynamic clusterization, and fully sufficient for acceptance, resolution, and background

Calorimeter components

NPS electromagnetic calorimeter

- 1200 $PBWO_4$ scintillators, PMTs + bases

SBS hadronic calorimeter

- 288 iron/scintillator detectors, PMTs + bases

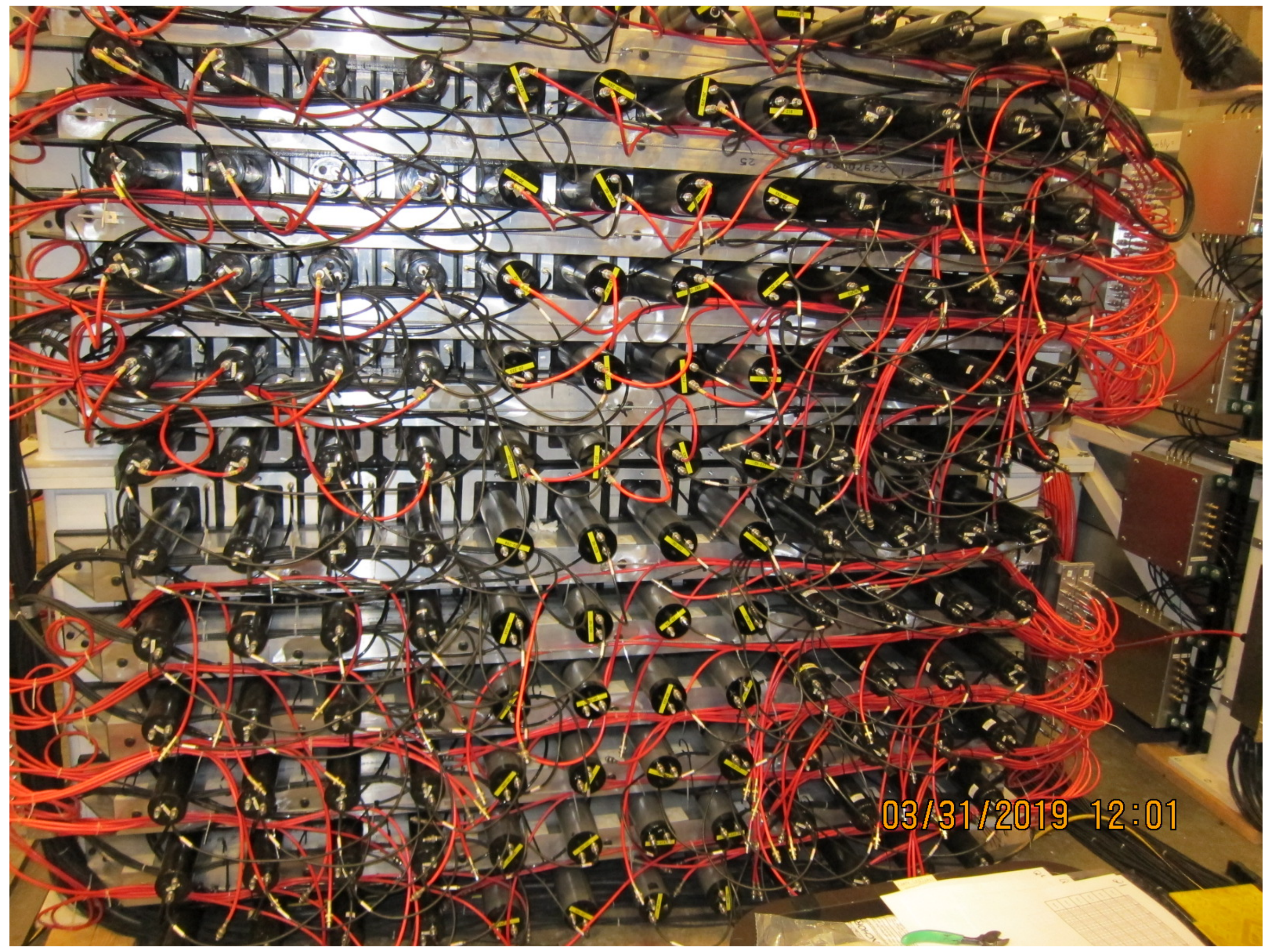

Scintillator Array

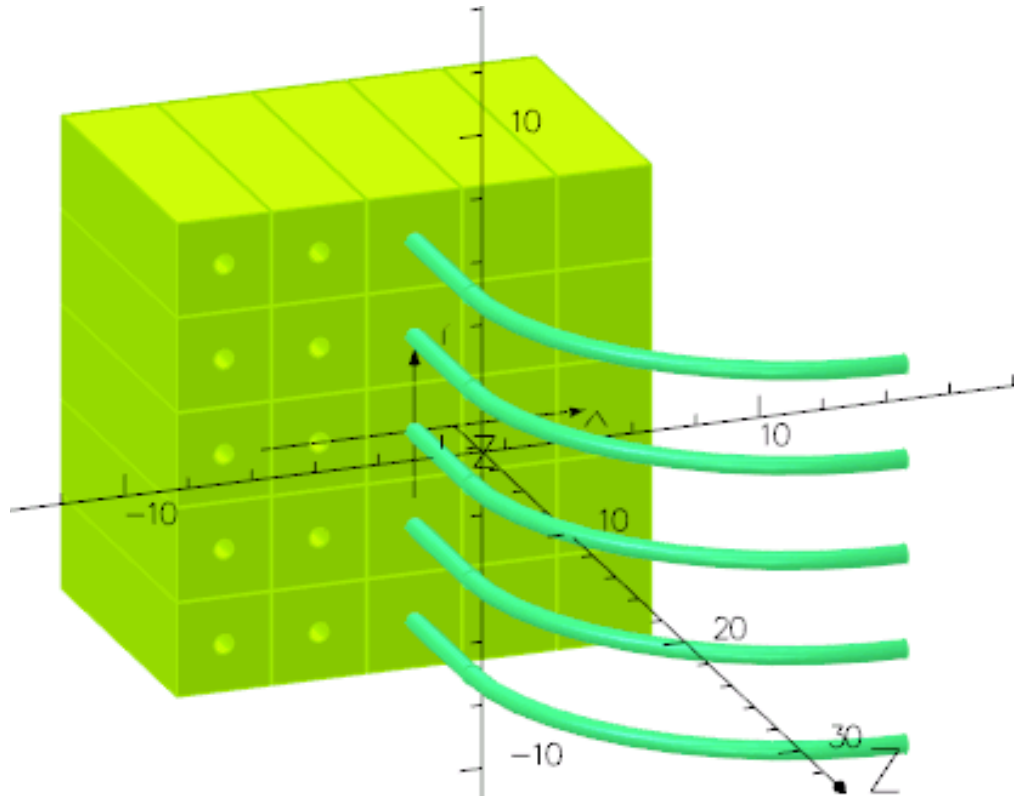

New detector to be built for this experiment
- Extruded plastic scintillator block
- Readout with wavelength-shifting fiber
- Each fiber read by pixel on multi-anode PMT
- 7200 blocks, each 3 x 3 x 10 cm^3
- Pipeline TDC readout (VETROC)

Q^2 dependence of Q^4F_1

$$F_1^u = 2F_{1p} + F_{1n} - F_1^s \qquad F_1^d = 2F_{1n} + F_{1p} - F_1^s$$

Assuming $\delta G^s_{E,M} \sim G_D \sim 0.048 \longrightarrow \delta(Q^4F_1^u) \sim \pm 0.17$

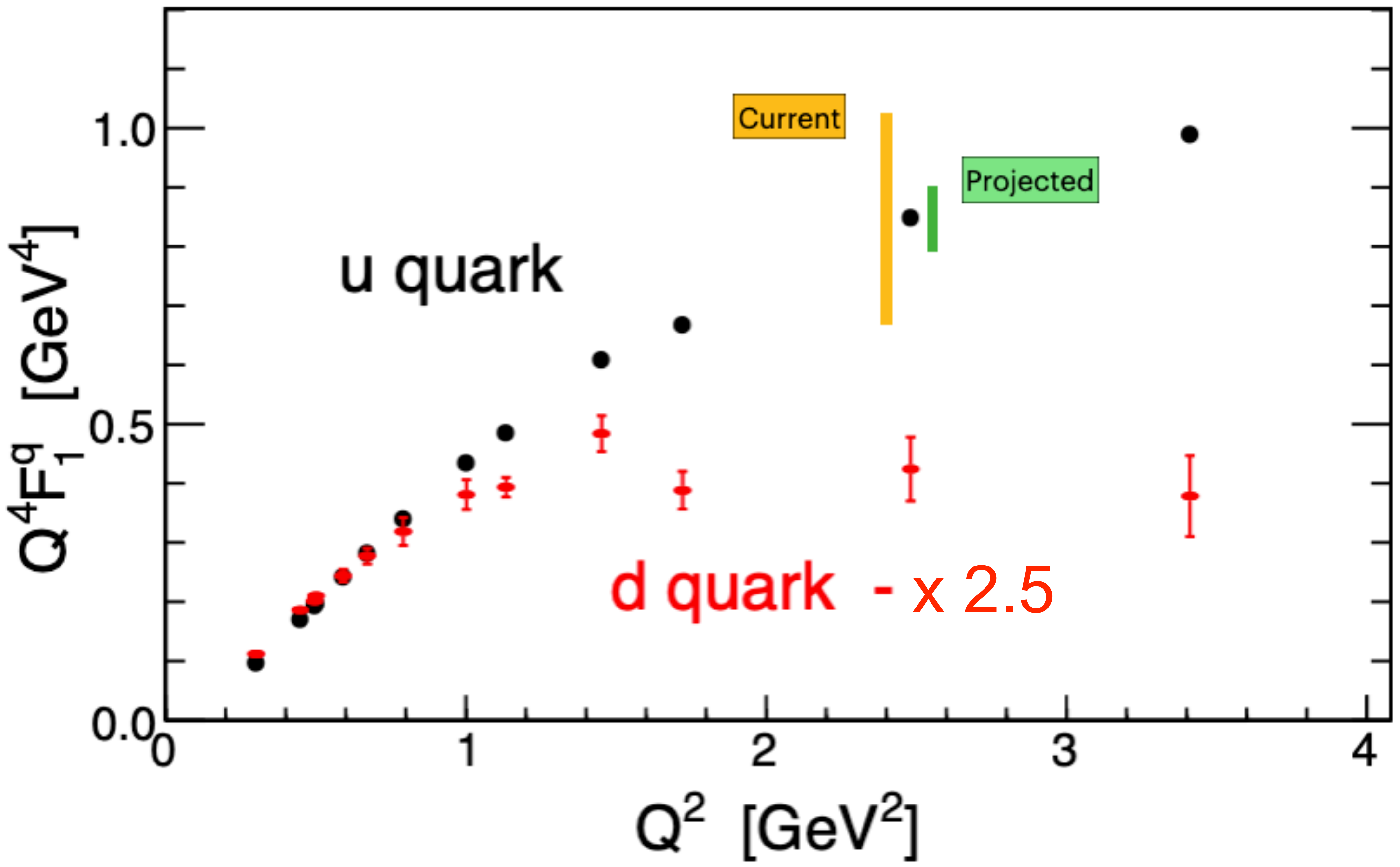

Such a large SFF could be huge in a proton PV measurement
$\delta A_{PV} \sim \pm 22$ ppm, ~±15% of A_{PV}^{ns}

- Flavor separated form factors are a crucial piece of information for GPDs / nuclear femtography.
- So far, these have relied on poorly tested assumptions of strange quark contributions.
- Experimentally not ruled out (at level of yellow band) and lattice calculations do not rule out significant contributions (at level of 1x-2x the green band)

A measurement is needed

Error budget

quantity	value	contributed uncertainty
Beam polarization	85% ± 1%	1.2%
Beam energy	$6.6 + / - 0.003$ GeV	0.1%
Scattering angle	$15.5^\circ \pm 0.03^\circ$	0.4%
Beam intensity	<100 nm,<10 ppm	0.2%
Backgrounds	< 0.2 ppm	0.2%
G_E^n/G_M^n	-0.2122 ± 0.017	0.9%
G_E^p/G_M^p	0.246 ± 0.0016	0.1%
σ_n/σ_p	0.402 ± 0.012	1.2%
$G_A^{Zp}/G_{\mathrm{Dipole}}$	-0.15 ± 0.02	0.9%
Total systematic uncertainty:		2.2%

or 3.3 ppm

Statistical precision for A_{PV}: 6.2 ppm (4.1%)

Radiative correction uncertainties are small; theoretical correction uncertainty lies in the proton “anapole” moment

If the anapole uncertainty is not improved, this would contribute at additional 4.1 ppm (2.7%) uncertainty

Scattering chamber

Cylindrical scattering chamber with large Al window to pass 15° electrons and 45° protons
Design uses a cone with "ribs", plus an inverted hemisphere center, windows could be as thin as 0.5mm

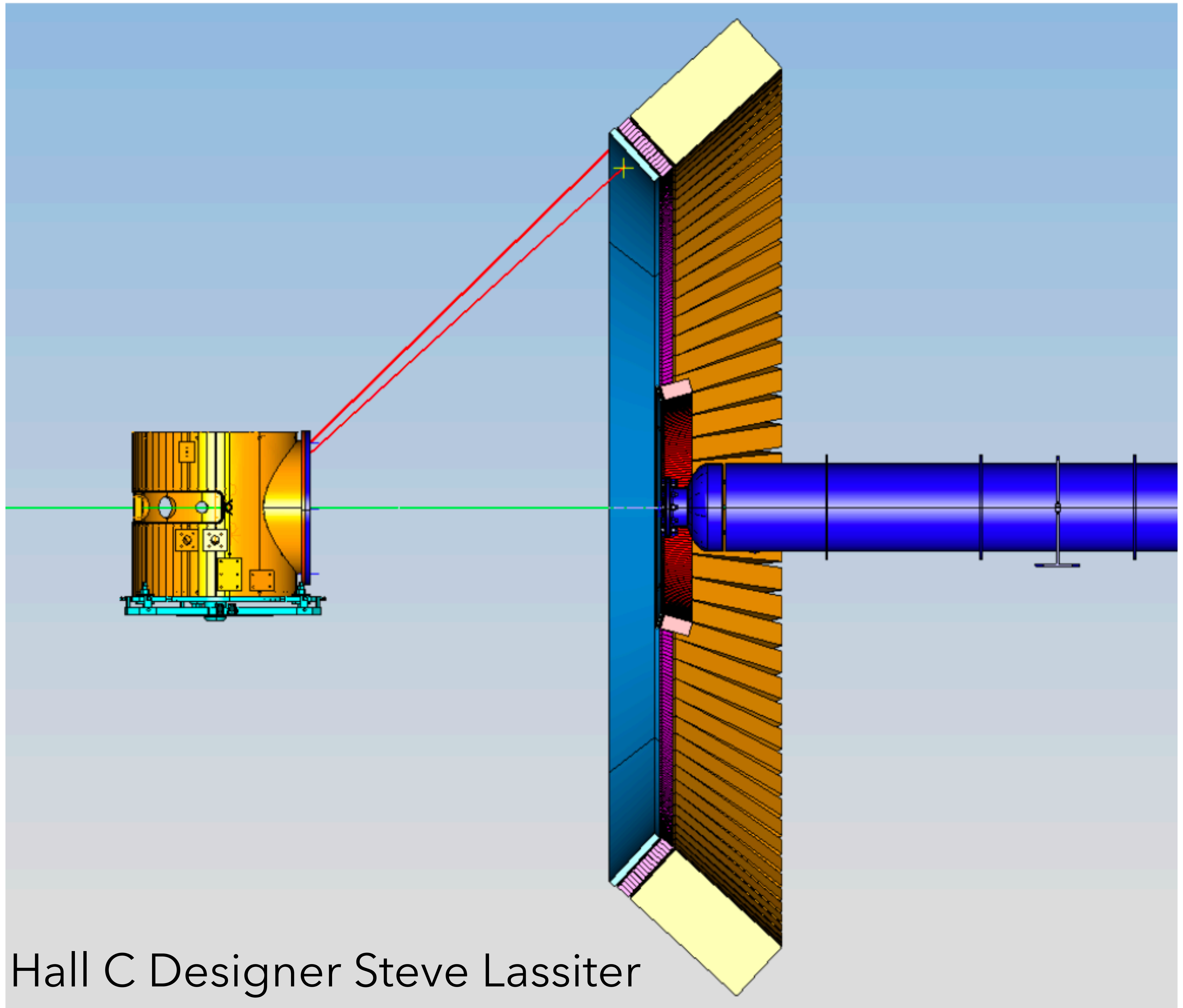

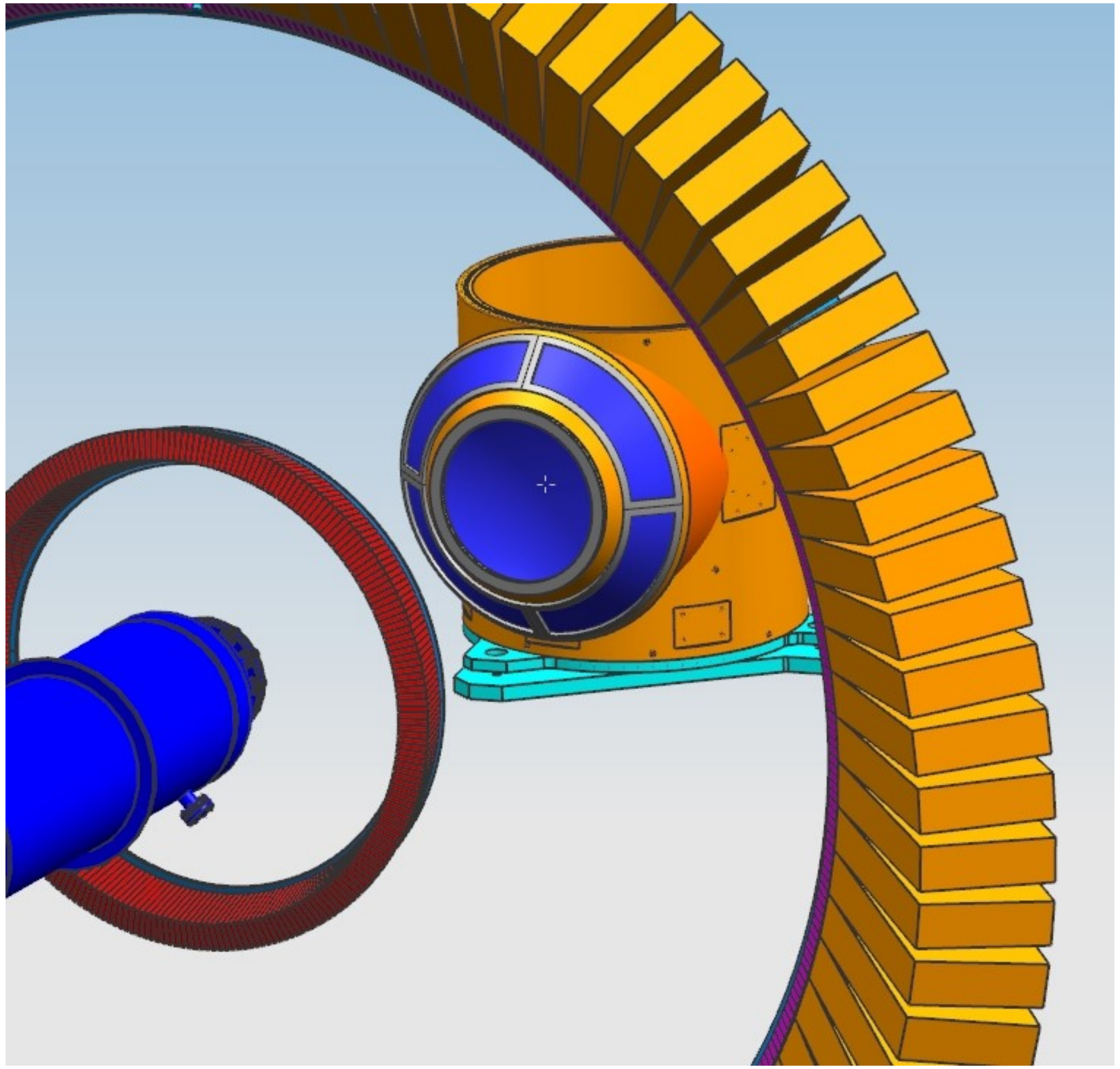

Requires air gap - will use He bag (not shown) to transport beam, so open air gap is only ~50cm